AEDC-TR-87-25
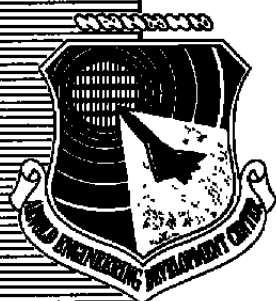
C-6

Thin Film Electret Bounday Layer Transition Detector (A Feasibility Study)

Roger C. Crites
Crites Enterprises
P. O. Box 13651
St. Louis, Missouri 63138

September 1987

Final Report for Period July 22, 1986 — January 22, 1987

ARNOLD ENGINEERING DEVELOPMENT CENTER
ARNOLD AIR FORCE BASE, TENNESSEE
AIR FORCE SYSTEMS COMMAND
UNITED STATES AIR FORCE

This report has been reviewed by the Office of Public Affairs (PA) and is releasable to the National Technical Information Service (NTIS). At NTIS, it will be available to the general public, including foreign nations.

APPROVAL STATEMENT

This report has been reviewed and approved.

ROBERT W. SMITH
Directorate of Technology
Deputy for Operations

Approved for publication:

FOR THE COMMANDER

MARION L. LASTER
Technical Director
Directorate of Technology

REPORT DOCUMENTATION PAGE

Form Approved
OMB No. 0704-0188

1a. REPORT SECURITY CLASSIFICATION UNCLASSIFIED	1b. RESTRICTIVE MARKINGS

2a. SECURITY CLASSIFICATION AUTHORITY	3. DISTRIBUTION/AVAILABILITY OF REPORT
2b. DECLASSIFICATION/DOWNGRADING SCHEDULE	Approved for public release; distribution is unlimited.

4. PERFORMING ORGANIZATION REPORT NUMBER(S) AEDC-TR-87-25	5. MONITORING ORGANIZATION REPORT NUMBER(S)

6a. NAME OF PERFORMING ORGANIZATION Crites Enterprises	6b. OFFICE SYMBOL (If applicable)	7a. NAME OF MONITORING ORGANIZATION

6c. ADDRESS (City, State, and ZIP Code) P. O. Box 13651 St. Louis, MO 63138	7b. ADDRESS (City, State, and ZIP Code)

8a. NAME OF FUNDING/SPONSORING ORGANIZATION Arnold Engineering Development Center	8b. OFFICE SYMBOL (If applicable) DOT	9 PROCUREMENT INSTRUMENT IDENTIFICATION NUMBER F40600-86-C0006

8c. ADDRESS (City, State, and ZIP Code) Air Force Systems Command Arnold Air Force Base, TN 37389-5000	10. SOURCE OF FUNDING NUMBERS			
	PROGRAM ELEMENT NO. 65502F	PROJECT NO.	TASK NO	WORK UNIT ACCESSION NO.

11. TITLE (Include Security Classification)
Thin Film Electret Boundary Layer Transition Detector (A Feasibility Study)

12. PERSONAL AUTHOR(S)
Crites, Roger, C., Crites Enterprises

13a. TYPE OF REPORT Final Report	13b. TIME COVERED FROM 7/22/86 TO 1/22/87	14. DATE OF REPORT (Year, Month, Day) September 1987	15. PAGE COUNT 45

16. SUPPLEMENTARY NOTATION
Available in Defense Technical Information Center (DTIC).

17.	COSATI CODES		18. SUBJECT TERMS (Continue on reverse if necessary and identify by block number)
FIELD	GROUP	SUB-GROUP	instrumentation transition
20	14		wind tunnel aerodynamics
			boundary layer

19. ABSTRACT (Continue on reverse if necessary and identify by block number)
A research task was conducted to determine the feasibility of developing an economical non-intrusive boundary layer transition detector. The new detector would be a thin (0.001 to 0.003 inch) plastic film with a large imbedded array of miniature fluctuating pressure transducers. Bonded to the aerodynamic surface of interest, the detector would yield a detailed map of fluctuating surface pressure. Turbulent bursts in the transitional region result in a characteristic peak in local surface pressure fluctuation. Transition would be located by resolving this peak. During this task, prototype transition detectors were fabricated. Thin film electret pressure transducer elements were used to form fluctuating pressure sensor arrays. A simple symmetrical wing model was fabricated and used to perform proof of concept testing in the University of Missouri-Rolla subsonic wind tunnel. The result of this wind tunnel test verifies the feasibility of developing thin film arrays of fluctuating pressure transducers, and of using these arrays to determine the location of boundary layer transition. Additional work is being planned to develop the technology necessary to allow rapid economical production of fluctuating pressure transducer arrays of almost any desired pattern and density.

20. DISTRIBUTION/AVAILABILITY OF ABSTRACT ☒ UNCLASSIFIED/UNLIMITED ☐ SAME AS RPT. ☐ DTIC USERS	21. ABSTRACT SECURITY CLASSIFICATION UNCLASSIFIED
22a. NAME OF RESPONSIBLE INDIVIDUAL C. L. Garner	22b TELEPHONE (Include Area Code) (615) 454-7813	22c OFFICE SYMBOL DOCS

DD Form 1473, JUN 86   Previous editions are obsolete.   SECURITY CLASSIFICATION OF THIS PAGE

PREFACE

The research work reported herein was proposed and conducted by Crites Enterprises of St. Louis, Missouri. The research was funded as an FY-1986 DOD SBIR project by Arnold Engineering Development Center (AEDC), Air Force Systems Command (AFSC), Arnold Air Force Base, Tennessee under Contract number F40600-86-C0006 during the period July 22, 1986 to January 22, 1987. Research, prototype development, and wind tunnel model fabrication were accomplished in St. Louis, using Crites Enterprises facilities. Feasibility, or proof of concept, testing was done in the University of Missouri-Rolla subsonic wind tunnel facility.

CONTENTS

ILLUSTRATIONS

Figure

1.0 INTRODUCTION

The boundary layer flow over the surface of a modern aircraft has a large effect on its aerodynamic characteristics. Therefore, an important aspect in the development of new flight vehicles is the determination of the effect of various design parameters on the boundary layer. In wind tunnel testing it is often desirable to monitor the boundary layer over various surface areas and determine whether it is laminar, transitional, or turbulent. Unfortunately, current methods of determining boundary layer transition are costly and often produce data of questionable interpretation.

The most common methods of detecting boundary layer transition are the hot wire anemometer and the surface total pressure probe. Hot wire anemometry was developed in the early nineteen hundreds for use in low speed wind tunnels. Modern electronics have improved the hardware considerably, and much work has been done to extend its range into the high speed compressible domain.[1,2,3] Nevertheless, the technique for measuring boundary layer transition is basically unchanged. An electrically heated wire is slowly moved along the surface of the model. The recorded signal is proportional to the current required to maintain the wire at a constant elevated temperature. As the wire moves from the laminar to transitional zones, turbulent bursts and increased diffusion cause a sharp rise in heat transfer rate. A good wire set has adequate frequency response to monitor the turbulence. A plot of turbulence level versus distance along the surface can be constructed and used to pick the transition location. One problem with this technique is that the presence of the hot wire disturbs the very flow it is measuring. Another problem is that it takes skilled and experienced personnel to successfully acquire and interpret the data.

Like the hot wire technique, the surface total pressure probe has been used for many years. Modern pressure transducers and data acquisition systems have improved the hardware. The range of application has been increased[3], but the method remains essentially unchanged. The probe slides along the surface of interest while total pressure is measured. The probe tip is usually flattened to create a vertical opening of 0.002 to 0.005 inches. The probe is started under the laminar boundary layer, and moved downstream into the turbulent boundary layer. As the transitional zone is entered the total pressure rises sharply due to increased momentum diffusion.

The transition location is usually specified as the point of maximum slope in the region of total pressure rise. This method is simple in concept and yields quantitative data that is easy to interpret. Unfortunately, the presence of the probe and its support and movement hardware create a large disturbance in the local flow field. This is particularly true in high speed tests, where the presence of the probe can cause shock waves which interact strongly with the local boundary layer. The surface total pressure probe is easier to use than the hot wire probe. It produces data that is easier to interpret than the hot wire probe. However, both methods can produce questionable data due to the interference of the probe with the local flow. For this reason a non-intrusive method, which does not insert a probe into the flow at the measuring point, is highly desirable.

There are several non-intrusive methods of measuring gas properties in a flowing environment. Most of these methods are optical in nature. With modern laser sources, photodetectors, and computer based data acquisition system, Raman scattering[4,5,6] resonant laser velocimetry[7] and aerodynamic holography[8,9,10] are relatively new and promising methods of non-intrusively measuring gas flow properties. Unfortunately, these methods are best suited to time averaged measurements of mean flow parameters, and (at this time) are not capable of both the spatial resolution and the frequency response necessary to accurately detect boundary layer transition.

The most widely used optical flow measuring method is the LV (Laser Velocimeter).[11,12,13,14] A rich and detailed methodology has developed around the use of the LV. In principle, the LV scatters laser light from "seed" particles, which for practical wind tunnel work must be introduced into the flow. The scattered light is collected and the velocity of the seed (presumably the same as the gas) is obtained from a sophisticated signal processor. The LV is capable of making good turbulence measurements. Spatial resolution, however, can be a problem. While the LV is easily the best of the optical tools available, it is not capable (at this time) of accurately mapping the boundary layer transition over a three-dimensional surface in a high speed wind tunnel.

Many investigators, such as Dougherty[15], have made boundary layer investigations using the surface total pressure probe with a closely coupled pressure transducer. As a result they can measure not only the mean total pressure, but the

fluctuating pressure. They report that as the probe passes through the transitional range, the fluctuating pressure increases sharply in magnitude, showing a well defined peak at the point of maximum slope in total pressure rise; i.e., at the point of transition. Local fluctuating pressure can therefore be used for boundary layer transition detection. Detecting boundary layer transition in this fashion offers no advantage because the probe still causes the same interference regardless of whether total pressure or fluctuating pressure is measured.

Wood, et al.,[16] in a very recent attempt to define candidate techniques for non-intrusive boundary layer measurements points to the use of fluctuating surface pressure. If pressure transducers could be flush mounted in the surface, in a streamwise line at close interval, the streamwise distribution of fluctuating pressure would identify transition. The problem with implementing this scheme is the time and cost involved in modifying the surface to accept many conventional pressure transducers.

Crites[17] invented a new kind of fluctuating pressure transducer. This transducer is the basis of an improved boundary layer transition sensor concept. The new transducer is fabricated from specially prepared layers of metallized plastic film. As a result it is very flexible and as thin as 0.001 inch. The improved boundary layer sensor would consist of an array of these transducer elements on a single plastic sheet. The sensor could be bonded directly to the surface of interest. It would be flexible enough to follow the local surface curvature, and thin enough not to trip the local boundary layer. Boundary layer transition would be detected by monitoring the RMS fluctuating pressure distribution over the transducer array, and resolving the transitional spike in intensity. We believe that this concept offers the best hope for economical non-intrusive boundary layer transition detection.

2.0 ELECTRET TRANSITION DETECTOR CONCEPT

An electret may be thought of as the analog of a magnet. A magnet is a material that produces a magnetic field at its surfaces in the absence of an external current source. An electret is a material that produces an electrostatic field at its surfaces in the absence of an external voltage source. The molecular structure of an electret material is polarized and aligned to produce a virtual "hetrocharge". This appears as a positive charge near one surface and a negative charge near the other. In the manufacturing process, ionic "homocharges" of opposite polarity are deposited on the surfaces. These charges are trapped by the internal field of the hetrocharge and produce a very strong electrostatic field in space near the electret. The actual phenomenology involved is complex[18], and beyond the scope of this report.

3

Electrets have been made from many different materials using many different processes. Early electrets were usually made from waxes[19] and were fairly thick. Modern electrets are made from very thin plastic film.[20] The thickness of modern electrets is typically on the order of 0.0003 to 0.0005 inch. Metallized K-1 Polycarbonate, and FEP Teflon were used to make electrets during the reduction to practice stage of the electret pressure transducer invention. Prototype transducers made with these electrets performed well. As noted by Sessler and West[21], electrets made from either of these materials will hold a net charge almost indefinitely.

Electrets have many applications, the most notable of which is the manufacture of microphones. Electret microphones are common place, having largely replaced condenser microphones because of superior performance and lower cost. They have also been given serious consideration for use in telephone transmitters.[22]

The conventional condenser microphone is essentially a capacitor formed by a metallic diaphragm and a metal backplate. A relatively high voltage is applied to charge this capacitor. Fluctuating pressure (sound) causes small movement in the diaphragm which changes the net capacitance and causes small voltage fluctuations to appear across the capacitor. The sensitivity of this arrangement depends on the quantity of charge stored in the capacitor. An electret microphone works the same way, except that the electret film replaces the metal diaphragm. Since the electret carries a permanent charge, no high voltage supply is necessary. The electret microphone doesn't need a power supply, it acts as a small generator, producing voltage fluctuations in response to pressure fluctuations.

Electret microphones have the sensitivity to measure surface pressure fluctuations. However, they are no easier to mount in the surface of a wind tunnel model than conventional transducers. The electret transducer element which is the basis of the electret transition detector concept avoids the rigid mechanical constraints inherent in conventional devices.

The electret transducer element is illustrated in Figure 1. A metallized plastic film, insulator/substrate, serves as the backplate. It can be directly bonded to the surface. The metallization serves as the active electrode. The signal is taken from it. The electret film is located a small distance above the substrate film with its metallization facing outward. The electret metallization is grounded, forming the other electrode of the capacitor, and a shield for the active electrode. The two metallized films are separated by an elastomer. The elastomer elastically deforms under pressure to vary the spacing between the two metallizations, and thereby vary the net capacitance. Since the capacitors net

4

charge is fixed by the electret, fluctuations is pressure
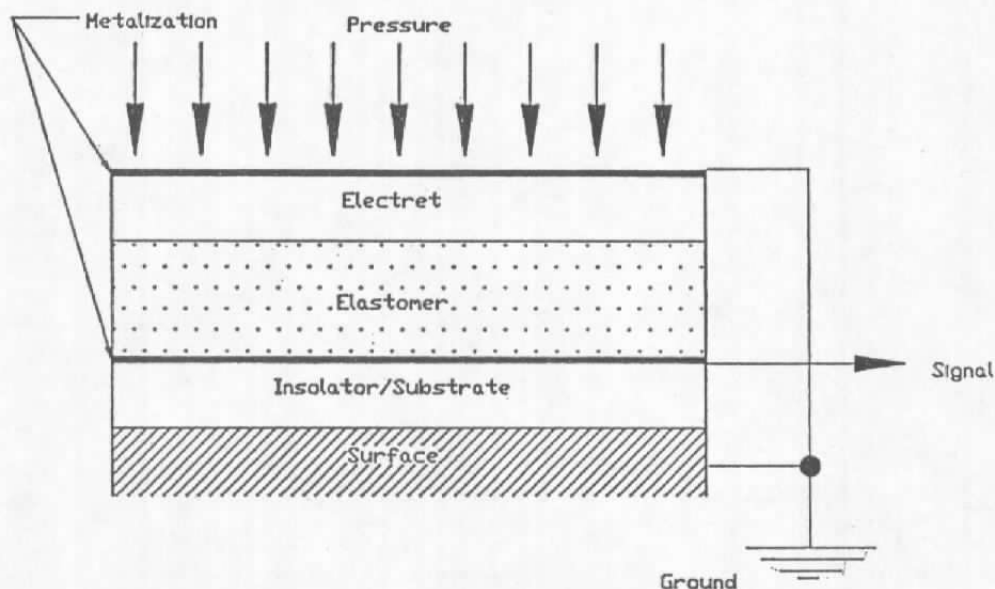cause corresponding fluctuations in voltage at the active
electrode.

Figure 1 - Basic Electret Transducer Element

The electret film and the substrate film are typically
about 0.0003 inches thick. Total transducer thickness depends
on the elastomer layer, but is typically between 0.001 and
0.003 inches. Mathematical modeling of this transducer
predicts some unique characteristics. The transducers dynamic
characteristics (to a first order approximation) are dependent
only on electret charge density and local elastomer
characteristics. Therefore, frequency response and
sensitivity are independent of size and shape. The transducer
element can have any convenient shape and size without
affecting dynamic characteristics. Another implication is
very high immunity to physical damage. A transducer element
can have small sections ripped away and the remains will still
function correctly.

Figure 2 is a comparison between the characteristics of a
prototype electret transducer and a conventional high response
instrument (Kulite). The electret transducer has a
sensitivity that is over twenty times greater than the Kulite,
and a roughly comparable frequency response.

The proposed boundary layer transition sensor will contain
many electret transducer elements in an array or matrix. In
its final form these arrays could contain hundreds of
individual transducer elements. Figure 3 shows a section of a
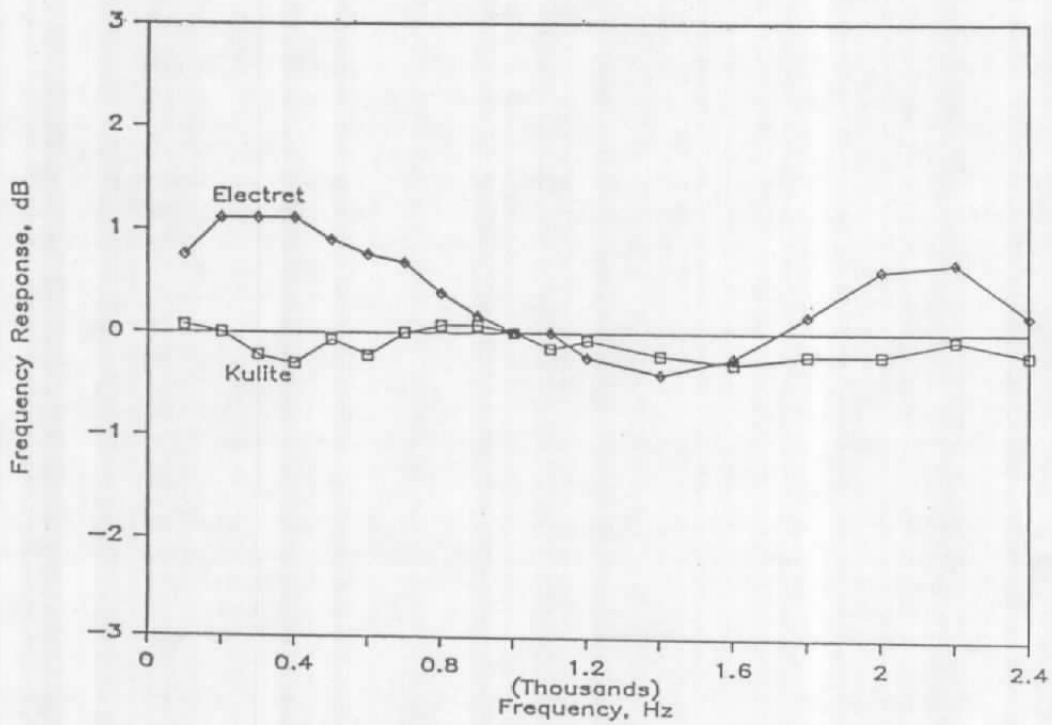possible electret boundary layer transition sensor. The
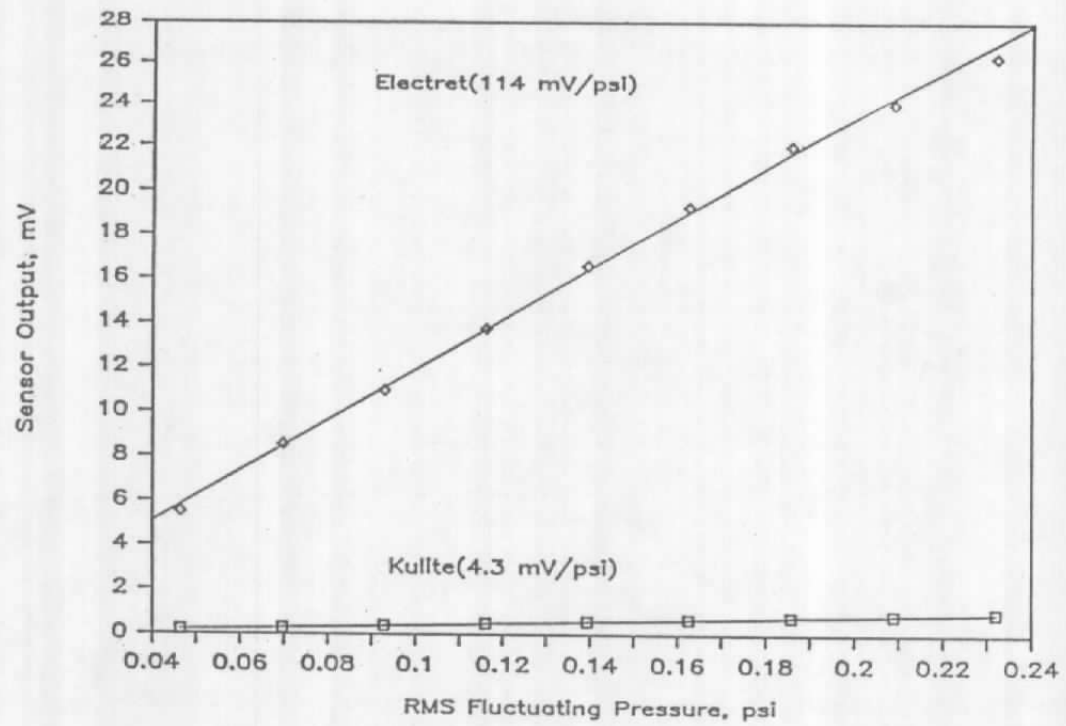
Figure 2 - Comparison of Typical Transducers

electret transducer elements are configured to maximize
resolution in the flow direction. Figure 4 illustrates the
application of this type of array. The array would be bonded
to the surface with the long axis of the sensor pads mounted
at right angles to the mean flow direction. For the example
given, this would yield a spatial resolution of 0.1 inch.

Figure 3 - Typical Transition Sensor Configuration
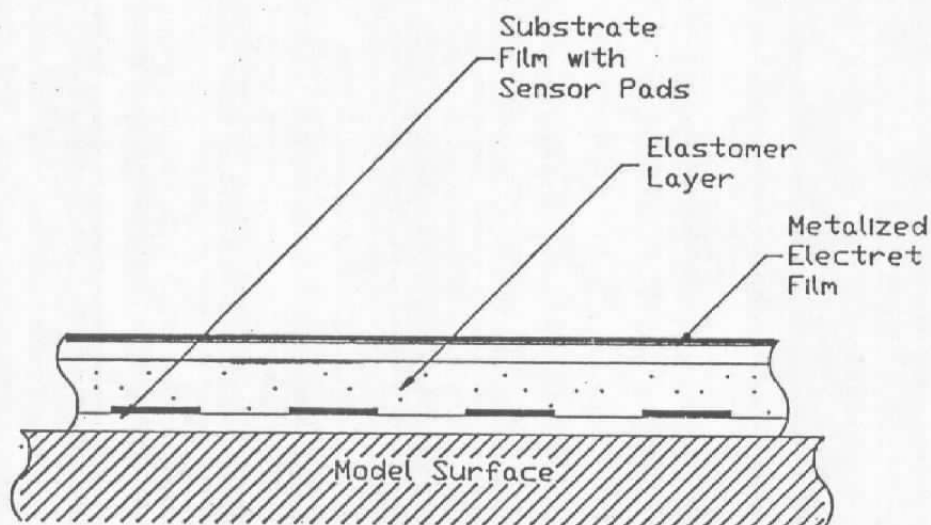
Figure 4 - Transition Sensor Cross-Section

3.0 FEASIBILITY STUDY

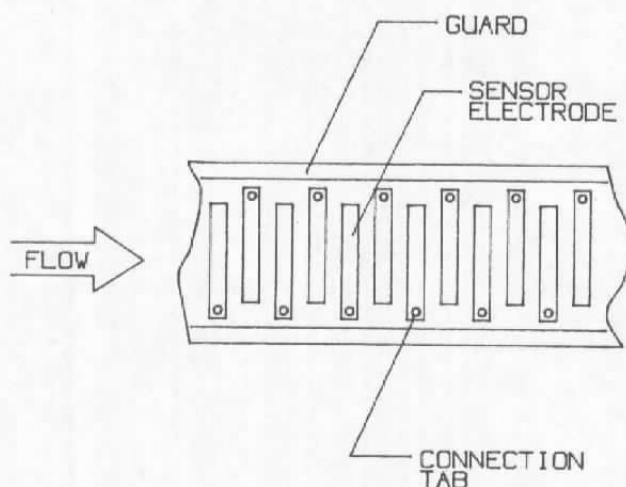A feasibility study, to determine the practicality of producing such electret transducer arrays, and of using them to locate boundary layer transition, was funded by the Air Force under a Phase I DOD SBIR contract. The research to be done under this contract was divided into four logical tasks. These are -

1. Electret Production
2. Sensor Fabrication
3. Model Fabrication
4. Wind Tunnel Testing

The work accomplished, and the results, for each of these tasks will be discussed in the remainder of this section.

3.1 Electret Production

Electrets were made by three separate processes. These are the "hot sandwich", Figure 5, the "hot ion spray", Figure 6, and the "cold ion spray", Figure 7.

Figure 5 - Hot Sandwich Process

OVEN

ION SPRAY

PLASTIC FILM

HIGH
VOLTAGE
DC

GROUND

Cu/CLAD
CIRCUIT
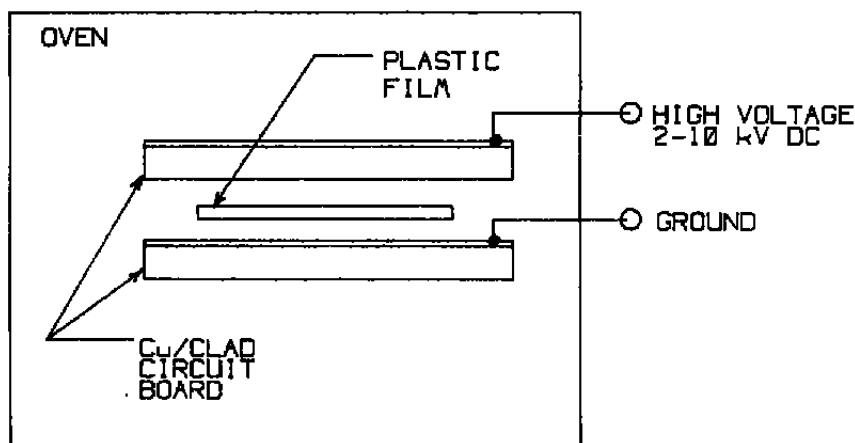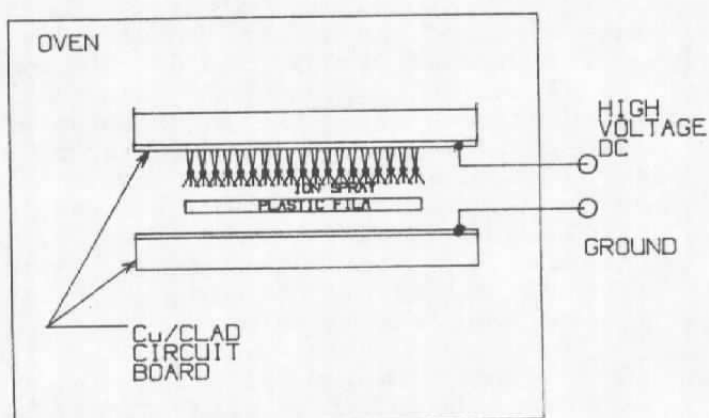BOARD

Figure 6 - Hot Ion Spray Process

HIGH
VOLTAGE
DC

CONTINUOUS
MOTION

ION SPRAY

PLASTIC FILM
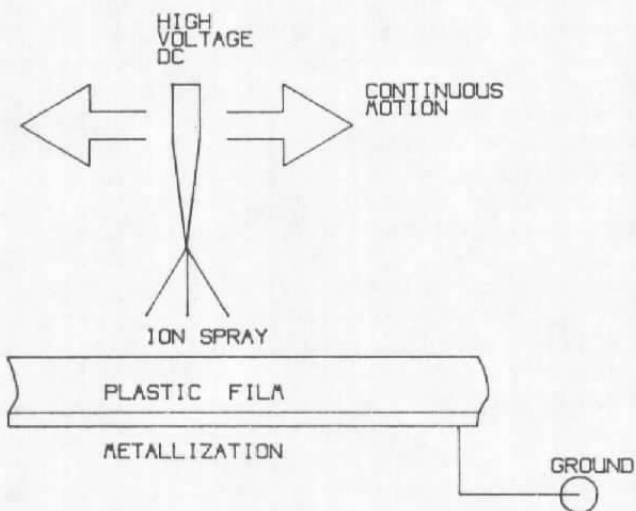
METALLIZATION

GROUND

Figure 7 - Cold Ion Spray Process

In the hot sandwich process the plastic film to be made into an electret is placed (metallization side down) on the copper surface of a Cu/clad circuit board. The epoxy side of another board is placed on top to form a "sandwich". A high voltage is applied while heating the sandwich in a laboratory oven. This creates an intense electric field through the sandwich. After soaking in this electric field at elevated temperature for about an hour, the oven is turned off. The sandwich is allowed to slowly cool while the polarizing voltage is maintained. When room temperature is reached the power supply is shut off and the plastic film, which is now an electret, is removed from the sandwich.

Care must be exercised in the selection of both the polarizing voltage and the soaking temperature. Initial attempts to use this electret activation process failed. Chromium metallized FEP Teflon was used for the electret material. A polarizing voltage of 2 kV, and a temperature of 350 deg.F. were selected (based on previous experience with this material). The result was that the chromium metallization was transferred from the Teflon film to the circuit board. It was found that with the batch of Teflon film obtained for this study, temperatures had to be limited to less than 250 deg. F. if damage was to be avoided. Previous work done with aluminized Teflon did not show this temperature limitation.

Since only the chromium metallization was available for this task, the temperature had to be limited. At the lower temperature it was found that 2 kV was not sufficient to produce strongly polarized electrets. The voltage was increased to 7 kV, at which time the circuit board insulation suffered dielectric breakdown. The resulting arc caused explosive delamination and destroyed the Teflon film. Figure 8 is a photograph of the copper side of the top circuit board in the sandwich. The copper cladding was separated from the epoxy and formed into a hemispherical bubble.

After some experimentation it was found that 6 kV at 240 deg. F. resulted in a strong polarization without damage to the metallization. A final refinement of the hot sandwich process was achieved by reducing the lateral dimensions of the circuit boards. Instead of polarizing a wide piece of film and then cutting it to the desired width, the film was cut to width (1.0 inch), and then polarized. The wider films were hard to keep wrinkle free while installing in the sandwich. Furthermore the heat would set the wrinkles, and cause creases in the metallization. It was often found that chromium migrated away from the creases so that electrical continuity was lost across the length of the film. By limiting the film width to 1.0 inch this problem was minimized.

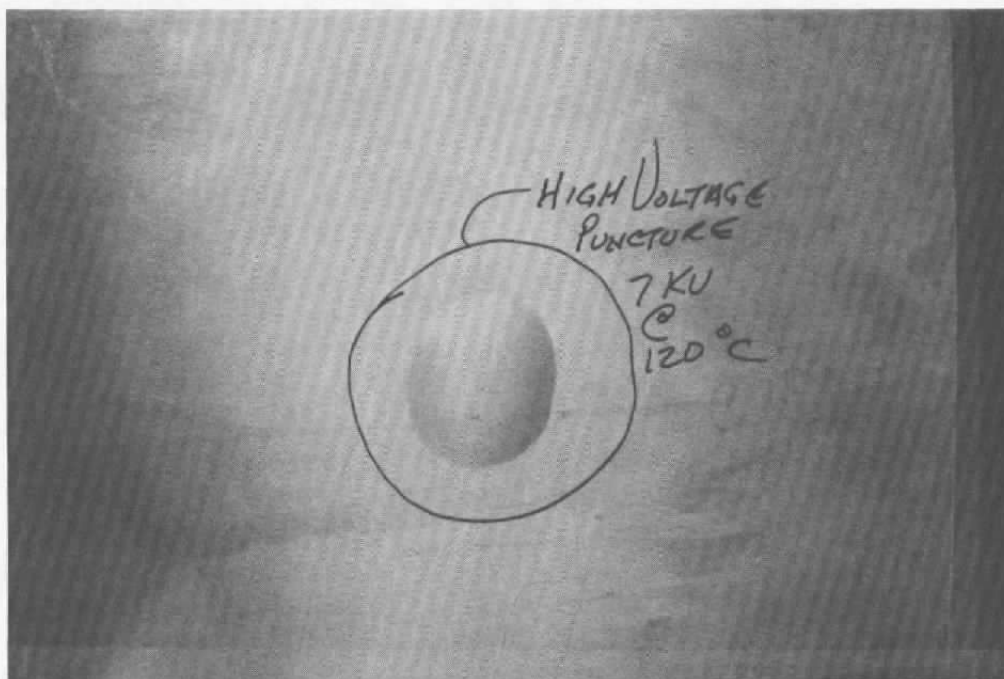Figure 9 is a photograph of the final hot sandwich implementation. Ceramic standoffs are used separate the
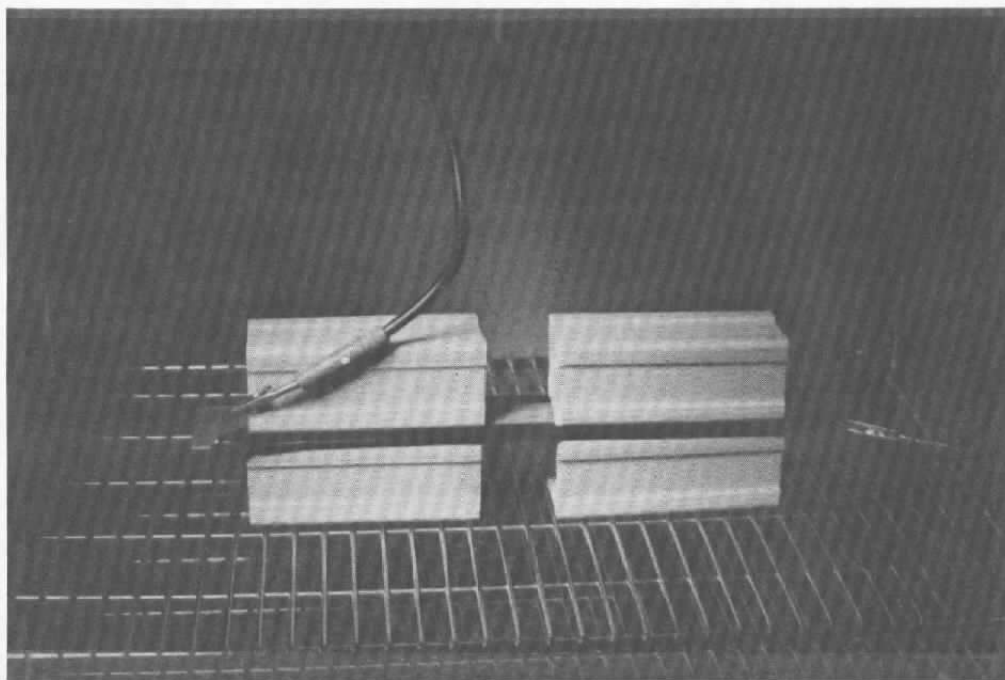
Figure 8 - Arc Damage

Figure 9 - Final Hot Sandwich Process

11

sandwich from the metal oven shelf. Additional standoffs are used as weights to keep the sandwich in position. After assembly, the edges of the sandwich are covered with electrical insulating tape. The purpose is to prevent corona discharge, and arcing from circuit board to circuit board at the edges.

Successful electret materials have polar molecular structures. This is illustrated in Figure 10. TFE Teflon cannot be made into an electret. Note the symmetrical molecular configuration. However, FEP Teflon makes excellent electrets. Note the asymmetrical molecular configuration, resulting in an asymmetrical charge distribution - a polar structure. There are two phenomena involved in the hot sandwich process. First, the intense electrical field tends to align the molecular electric dipoles - which once aligned tend to be self sustaining. Supposedly the heat aids in the realignment process. Second, there is a thin layer of air trapped between the top of the sandwich and the plastic surface of the film. Since the dielectric constant drops abruptly at the epoxy/air interface, the local field strength rises sharply - ionizing the air in the gap. These ions are accelerated into the surface of the plastic film and trapped there. The net electret charge is the superposition of the aligned components of the molecular electric dipoles and the trapped surface charge.
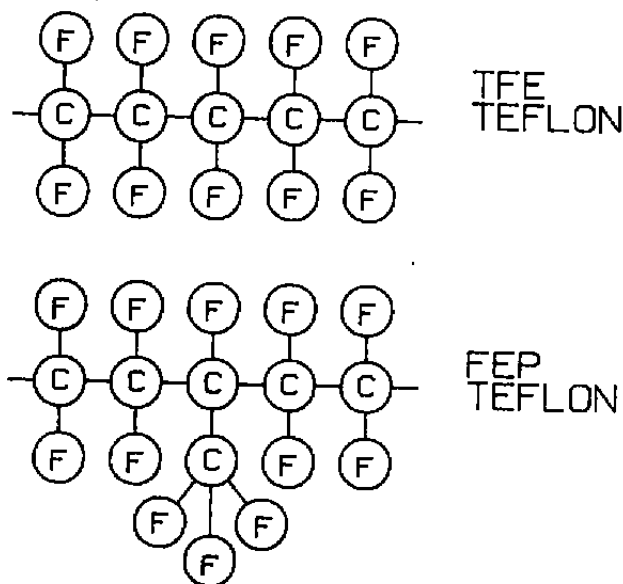

Figure 10 - Electret Materials

In the electret samples made with the hot sandwich
process, the surface charge seemed to dominate. The hot ion
spray process was developed in an attempt to increase the
trapped surface charge. Figure 11 is a photograph of the hot
ion spray process of making electrets. The plastic film to
become an electret is cut to width (1.0 inch) and taped -
metallization side down - to a copper plate. Quarter inch
thick Teflon blocks are placed at each end of the plastic
film. A specially prepared piece of Cu/clad circuit board is
positioned on these Teflon blocks. This board has many small
needle points soldered to the copper side. The needles point
down - at the plastic film. Ceramic standoffs are used to
weight the ends and hold the components in alignment.
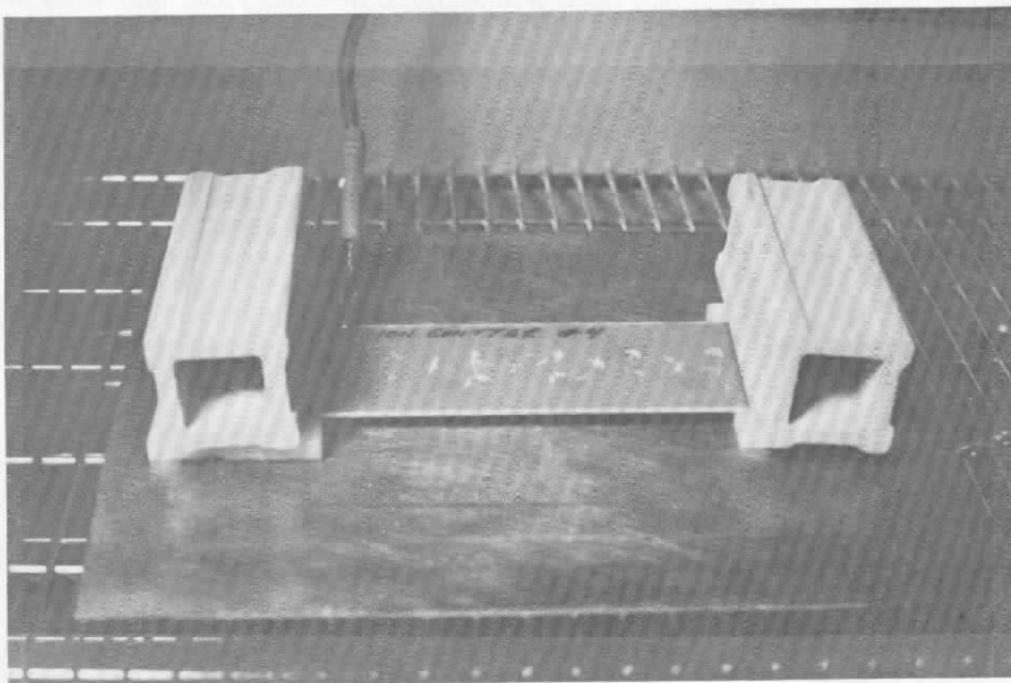
Figure 11 - Hot Ion Spray Process

In use, the bottom copper plate is grounded and the top
board with the needle points (the ion emitter) is connected to
a high negative voltage supply. The needle points cause a
local intensification of the electric field sufficient to
cause ionization of the air - a corona discharge. The field
accelerates ionic charge into the plastic film.

In practice this method worked, but not well. The process
was unstable. That is, it would spontaneously arc - burning
holes through the plastic film. The voltage would be slowly
increased until the desired ion current was obtained. All
would be well for an indeterminate period (from seconds to
several minutes). Then an arc would occur, destroying the
electret. The problem seemed to be associated with the

13

accumulation of space charge in the gap between the ion
emitter and the plastic film. It is hypothesized that the ion
density in the gap increased, decreasing the dielectric
strength of the air, until breakdown occurred. This process
was abandoned.

The cold ion spray process was developed to accomplish the
purpose of the hot ion spray process - increase the net
surface charge - and avoid the unstable arcing associated with
the accumulation of space charge in the gap. This was done by
making an improved ion emitter which consisted of a row of
tiny, very sharp, needles. The width of the row of needles
was slightly larger than the width of the plastic film to be
processed. To prevent space charge accumulation the emitter
would be continuously moved back and forth over the length of
the plastic film. Experimentation indicated that heat was not
necessary to accomplish charge capture at the plastic films
surface. Therefore the oven was eliminated.

Figure 12 is a photograph of the cold ion spray
apparatus. The plastic film is laid in the bottom of a slider
channel and secured with tape. The metallization is down
against a glass bottom, and is grounded. Shims are laid in
the channel to cover the edges of the film and to serve as a
slider bearing. The ion emitting needles are held in a slider
which rests on the shims. A brush contact on the slider
connects the needles to a high voltage supply.

Figure 12 - Cold Ion Spray Process
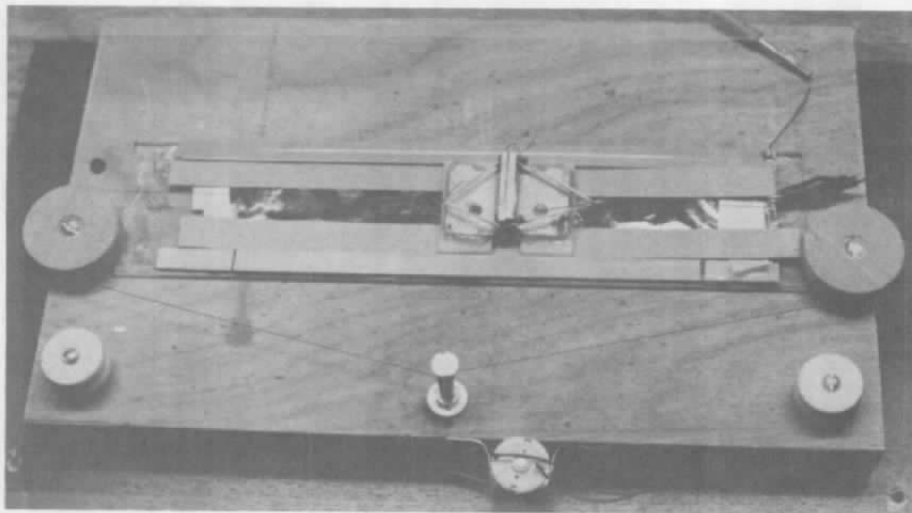
A small DC motor drives a capstan which moves the slider at
a constant speed over the surface of the film. When the
slider reaches one end of the channel the motor is reversed
driving the slider toward the other end of the channel. Since
the emitter is in constant motion, there is no significant
accumulation of space charge, and the spurious arcing of the
hot ion spray is avoided.

Electret material was made from chromium metallized FEP
Teflon and from aluminized Mylar. Electrets were made using
both the hot sandwich and the cold ion spray processes.
Charge density and stability was periodically measured to
determine which electret process was best.

Measurements were made using an improved separable
capacitor method. This method is illustrated in Figure 13.
The electret film is placed (metallization down) on a copper
plate. The copper plate is grounded. A copper probe of known
area is placed on the top of the electret. The probe and the
metallization of the underside of the electret form a
capacitor. Since variation in the air film trapped under the
probe can result in small changes in capacitance, the
capacitance is measured using a sensitive electronic
capacitance bridge. The probe is then grounded. Current
flows between the electret metallization and the probe until
the charge on the probe balances the field at the surface of
the electret. The probe is then connected to a calibrated
capacitor of known capacitance, and quickly lifted from the
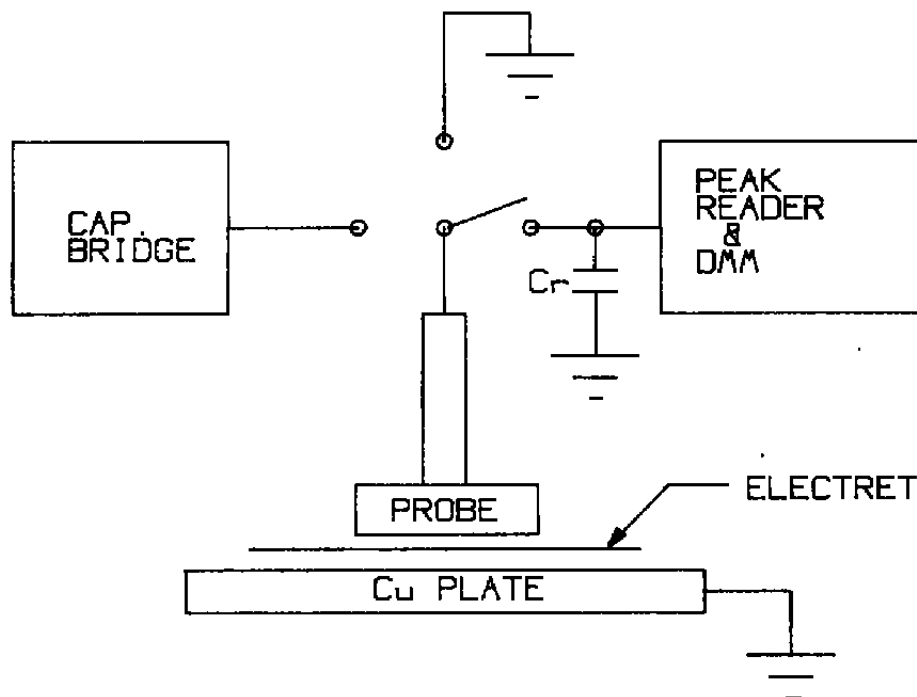
Figure 13 - Charge Density Measurement

surface of the electret. As the probe lifts, its capacitance drops to a negligible value and the charge is transferred to the calibration capacitor. A peak reader circuit records the voltage developed on the calibration capacitor.

Measurements made by this method show the charge density for electrets made by either method to be of the order of 10^{-8} C/in^2. There seemed little to recommend one electret process over the other. Later, during the fabrication of sensors for the wind tunnel test, the electrets were moved from an unheated area to a warm area. Water condensation occurred on the electrets. It was subsequently discovered that only electrets made of Teflon by the hot sandwich process retained a strong charge. Therefore only these electrets were used for the wind tunnel test. Further investigation is needed to determine the cause of damage, and establish adequate preventative measures.

3.2 Prototype Sensor Fabrication

As shown previously, the sensors consist of three basic components. First is the substrate - an insulating plastic film with a conductive metallization on one side forming the sensor electrodes and possibly connecting leads. The second is the elastomer layer - an insulating compressive separation between the substrate layer and the the electret (which is the last layer). In addition there are the adhesives needed to hold the laminates together, and to the surface of interest.

The material selected for the substrate was 0.25 mil aluminized Mylar. A very efficient method was developed for obtaining the required metallization patterns. The conductive areas (sensor electrodes and connector tabs) were drawn using a PC CAD system. Plotter pens were modified to contain a chemical resist ink. Sheets of Mylar were taped to plotter paper, metallization up. The desired conductive patterns were then plotted full scale using the resist pens on the Mylar. The Mylar sheets were then subjected to an electrochemical etching process which removed all metallization not covered by the resist ink. Following etching, the Mylar sheets were washed in isopropyl alcohol, which removed the resist ink - leaving the desired metallization pattern.

Substrate patterns were generated for test plates, containing 4 sensor elements. Substrate patterns were also generated for the wind tunnel test. These were about 6 inches in length. Two sensor densities were developed. These were 10 sensors per inch, and 5 sensors per inch. The test plate patterns were generated in the same two densities.

For the proof of concept testing it was decided to build the sensors up directly on the test surface. Developing the sensor matrix as a tape to be applied to the surface involves production problems beyond the scope of a feasibility study. The first step in the sensor assembly development was to find a proper adhesive for bonding the substrate to the test surface.

After consulting with several adhesive experts, S707 Plastilock (BF Goodrich Company) was selected as the proper adhesive. This adhesive comes in a spray can. With much practice, a technique was developed for spraying a thin uniform coat of adhesive and applying the substrate. The results appeared acceptable. Adhesion was excellent.

Electrically conductive cements are used to connect the instrumentation leads to the sensor pads. Curing at elevated temperatures is desirable to reduce the cure time. Also it is desirable to "age" (temperature cycle) the completed sensor assembly to increase stability of the sensor characteristics. Therefore samples of test plate substrates were bonded to plexiglass and submitted to temperatures anticipated for the conductive adhesives and for aging of the sensors.

The results were disappointing. At about 130 deg.F the S707 began to break down. Figure 14 is a photograph of a test plate 5/in. substrate after being subjected to a temperature of about 135 deg. F. After some experimentation a cyanoacrylate (Duro Super Glue) adhesive was selected. Figure 15 is a photograph of a 5/in. test plate bonded to plexiglas after exposure to 180 deg. F. The cyanoacrylate was used on all subsequent prototype sensors for bonding the substrate to the surface. According to Loctite Corp. (the manufacturer) cyanoacrylate has very low toxicity and produces no dangerous thermal decomposition products. Figure 16 is a photograph of a 10 transducer per inch substrate with 60 transducers bonded to a plexiglas plate.
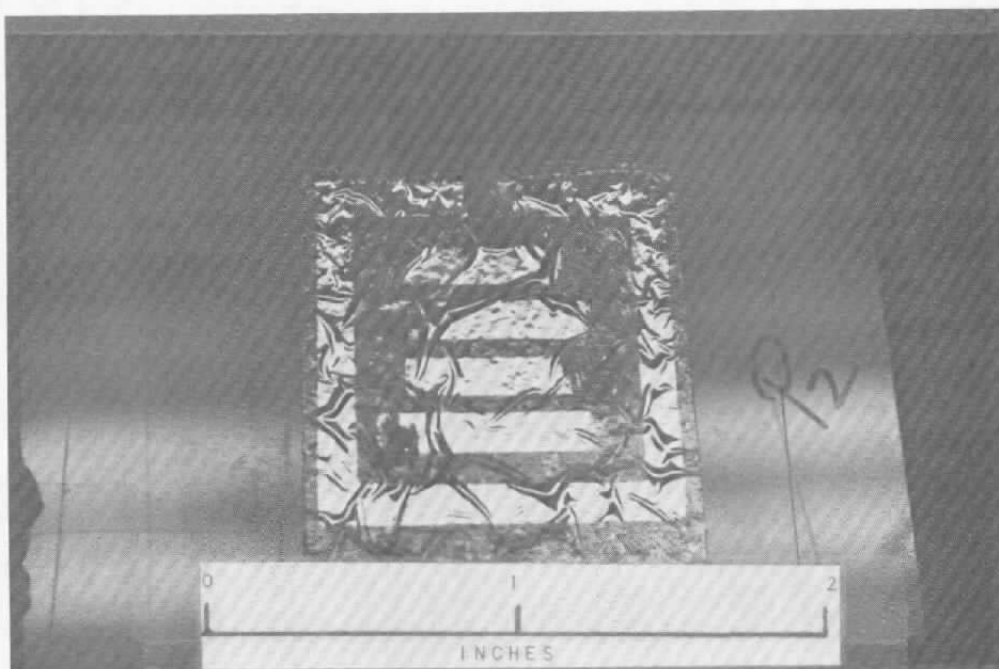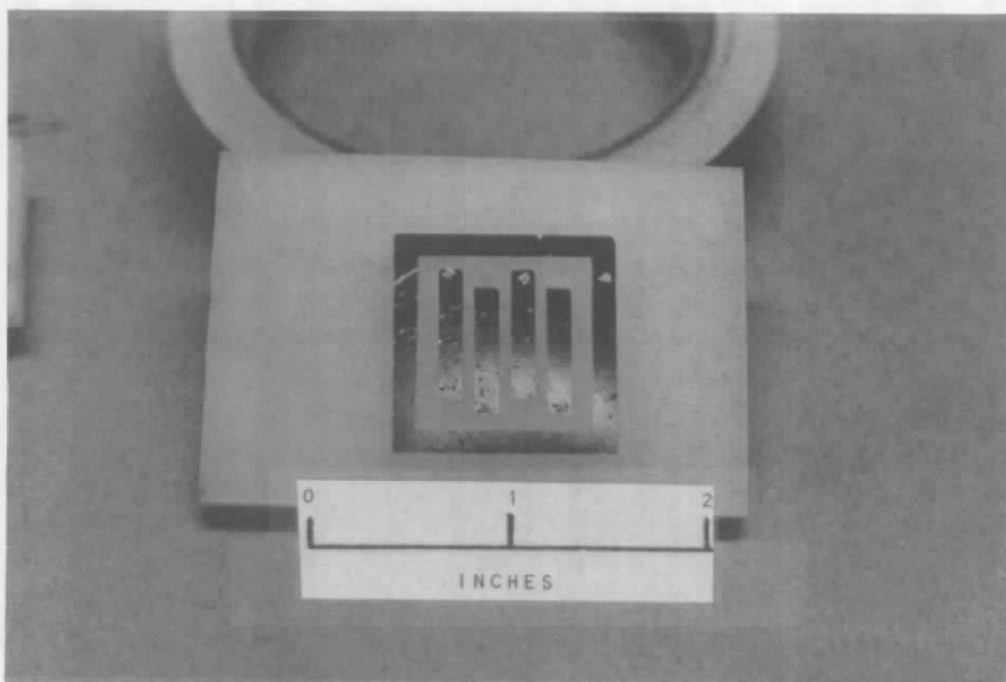

Figure 14 - S707 Adhesive Failure
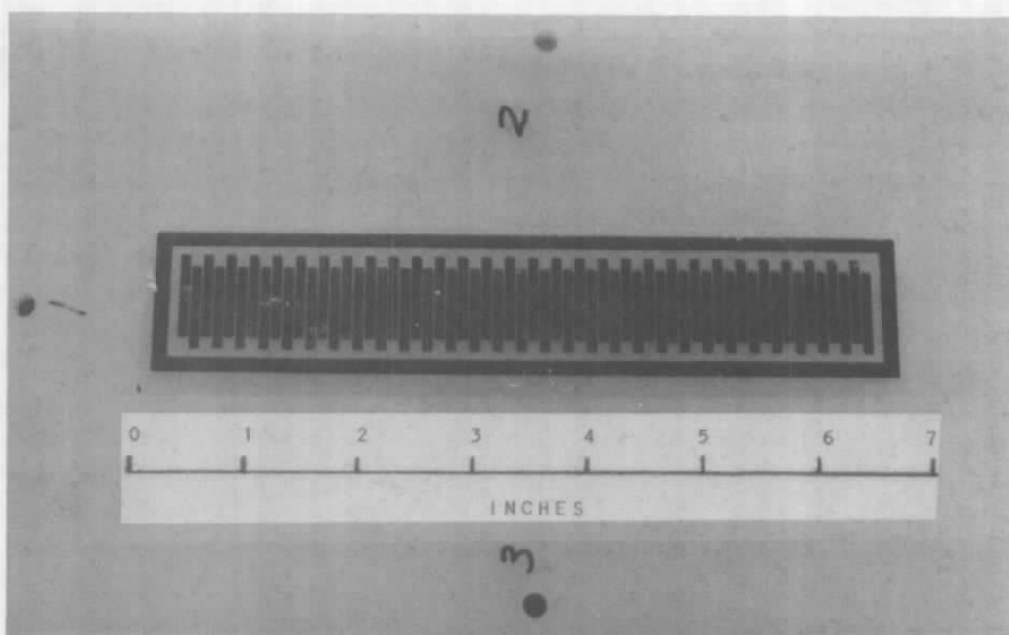
17

Figure 15 - Cyanoacrylate Success

Figure 16 - 60 Transducer Substrate @ 10/in.

For the feasibility test it was decided to drill a small hole through the sensor attach tabs and right on through the surface. Signal leads were passed through the holes from the bottom, and bonded to the sensor tabs. Two different adhesives were obtained for this. The first was ME-101 (Thermoset Plastics Inc.) conductive epoxy. This is a microelectronic grade, silver filled, epoxy. The other adhesive was CF-1525 Electrically Conductive Silicone (McGhan NuSil Corp.).

Figure 16 is a photograph of an electret sensor substrate with 60 transducer elements. This is an example of the 10 transducer per inch pitch. The attach tabs are simply staggered extensions of the sensor electrodes. The staggered arrangement allows greater clearance when attaching the signal leads. The metallization that surrounds the sensor electrodes and attach tabs is a guard ring. The electret material is trimmed so that the edges of the electret material lie on this guard ring. The metallization on top of the electret is then electrically connected to the guard ring with conductive adhesive. This provides the ground connection and top shield connection.

In the final form, the electrical connections for the sensors would be carried on the substrate to a convenient remote termination. Again, for a feasibility test, this involves development efforts that are unwarranted. For the proof of concept wind tunnel test a much simpler approach was chosen. The procedure is illustrated for a single sensor attach tab in Figure 17. A small hole is drilled through the attach tab and on through the surface. A small length (0.1 inch) of insulation is stripped from one end of the signal wire, and the wire is inserted until the ends of the bare wire are just below the surface. A conductive adhesive is then used to bond the wire in place, and to make electrical contact between the wire and the sensor electrode.

Two different adhesives were used for this purpose. The first is ME - 101 (Thermoset Plastics Inc.). This adhesive is a two part microelectronics grade, silver filled epoxy. The other was CF-1525 (McGhan NuSil Corp.). This adhesive is a three part platinum system, silver filled silicone. Both adhesives were used to make prototype sensors. The ME - 101 epoxy has the advantages of simpler mixing and use, simpler handling, faster cure cycle, and superior adhesion. It has one disadvantage - it is not conductive until it has cured. Therefore, the quality of electrical connections cannot be determined while the adhesive is being applied. The CF - 1525 requires a much longer cure cycle, is more difficult to mix, harder to apply, but is conductive as mixed. Therefore the integrity of each connection can be determined as it is being made.
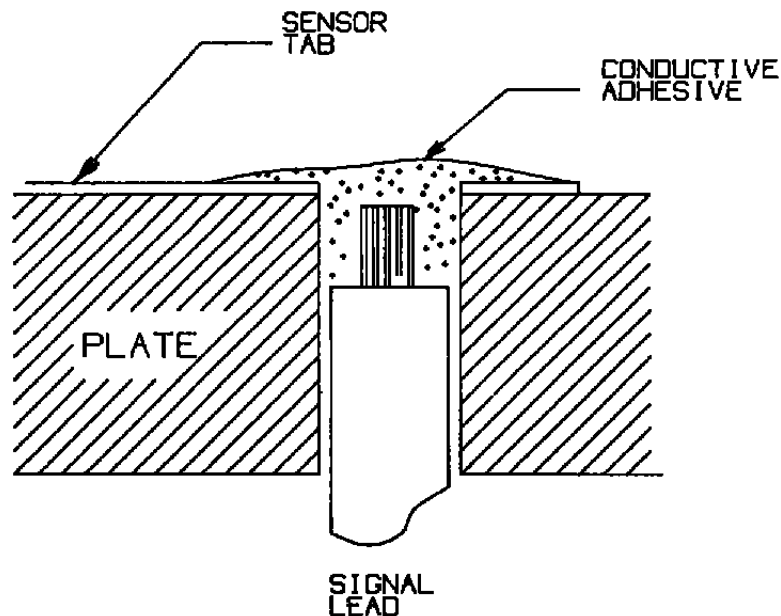
SENSOR
TAB

CONDUCTIVE
ADHESIVE

PLATE

SIGNAL
LEAD

Figure 17 - Typical Sensor Connection

The next component of the sensor to be applied is the elastomer layer. It was hoped that an elastomer could be found that would also serve as the adhesive for the electret layer. CSL 506 and CSL 588 (CSL Silicones Inc.) electronic grade RTV silicones were obtained and evaluated. These are one part, noncorrosive materials. They are easy to apply, and show good compliance (low stiffness). Unfortunately three problems were discovered. First, cure time (in the electret transducer element) appeared to be in excess of a week. For a 6 month feasibility study this is much to long to allow reasonable development time. The second problem was adhesion. The material demonstrated good adhesion to the Mylar substrate, but not to the Teflon electret.·

The third problem had to do with the elastic properties of the material. Both CSL588 and CSL 506 showed very high damping. The restoring force appeared to be a function of the rate of deformation. If this material were used for the elastomer layer it would result in a badly distorted frequency response. The time constraints of the contract did not permit the search for elastomer materials to begin over. A compromise had to be found.

It was discovered that the elastic properties of the CF-1525 electrically conductive silicone were superior to those of the CSL silicones. The elastic modulus of CF-1525 was, however, greater than desired. To increase the compliance, a matrix of air pockets was created in the elastomer. Great care was taken to insure that no conductive path existed between sensor electrodes. Adhesion to the Teflon electret material was poor. However adhesion to the metallization on the top of the electret was very good. Since the electret was secured along its edges by bonding the chromium metallization to the guard ring, there was no danger of delamination.

The sensitivity of trial electret sensors of this design was on the order of 100 mV/psi. The wind tunnel testing was to be conducted primarily at dynamic pressures of 2 inches of water (0.072 psi) and 4 inches of water (0.144 psi). Fluctuating surface pressure was expected to be on the order of 1 percent of the dynamic pressure. Therefore RMS pressure levels of the order of 0.001 psi were expected. With a sensitivity of only 100 mV/psi the signal level would be on the order of 0.1 mV. There was no way to estimate the electrical background noise in the wind tunnel. However it appeared that signal to noise levels might be poor.

In order to boost the sensitivity, two new sensor designs were implemented. These designs use only air as the compressive material in the elastomer layer. Both of these designs use Mylar (no metallization) to form a mask. The mask is attached to the top of the substrate in place of the elastomer layer. The mask supports the electret above the substrate. In the segmented air layer design the mask exposes the sensor electrodes, but fills the gaps between them. The electret is supported on all sides of each transducer element. Since the Mylar does not compress (at the pressures being considered here), the result is that each transducer element is isolated and independent.

The other design is called the continuous air layer design. This is similar to the segmented air layer design except that the Mylar mask does not fill the gap between the sensor electrodes. The Mylar mask runs lengthwise along the entire sensor, but does not isolate the air layers between sensor elements. Therefore, the elements of the sensor are not independent. The signals from this design should represent a smoothed pressure field.

Prototype electret boundary layer transition sensors were fabricated for the wind tunnel test from all three designs. As explained in the next section, prototype sensors were installed on plexiglas test plates. These plates were formed to the surface contour of the wind tunnel model. The plates could be rapidly changed without removing the model from the wind tunnel. All of the prototypes for the wind tunnel test used the 5 transducer per inch pitch, and contained 30 sensor elements.

Plate 1 used the segmented air layer design. Plate 2 used the continuous air layer design. Plate 3 used the air in elastomer matrix design. As explained in the previous section, chromium metallized FEP Teflon electrets were used on all three plates.

Evaluation of individual electret transducer elements was accomplished in the calibration set up illustrated in Figure 18. A single transducer element of the design to be evaluated was bonded to the end cap of a standing wave tube. A miniature microphone of known characteristics is also mounted flush in the same end cap. This microphone serves as a reference standard for the calibration. Sinusoidal pressure oscillations are generated in the standing wave tube by a 30 Watt acoustic driver. Frequency and amplitude are variable. The standing wave tube can calibrate a device over a wide frequency range at sound pressure levels characteristic of surface pressure fluctuations in low speed wind tunnels. At specific resonant frequencies, sound pressure levels characteristic of transonic and supersonic wind tunnels can be achieved.

The wave mode is monitored using a dual beam scope (Figure 19) to insure that the wave front in the chamber is planar. At very high frequencies the wave front is perturbed by higher resonant modes and the sound pressure level is no longer constant over the entire end cap. If calibration is required under these conditions, a reciprocity technique can be used. Simply speaking, a reading is taken, the end cap is rotated 180 degrees to swap positions of test device and standard, and another reading is taken.

Obviously this calibration setup is not directly applicable to the calibration of a sensor which is 6 inches long and contains either 30 to 60 individual transducers. To perform electret transition sensor calibrations it was necessary to transfer the calibration to the standing wave tube itself. This was done by mounting a reference standard microphone flush in the surface of a plexiglas plate as shown in Figure 20. Another reference standard microphone was
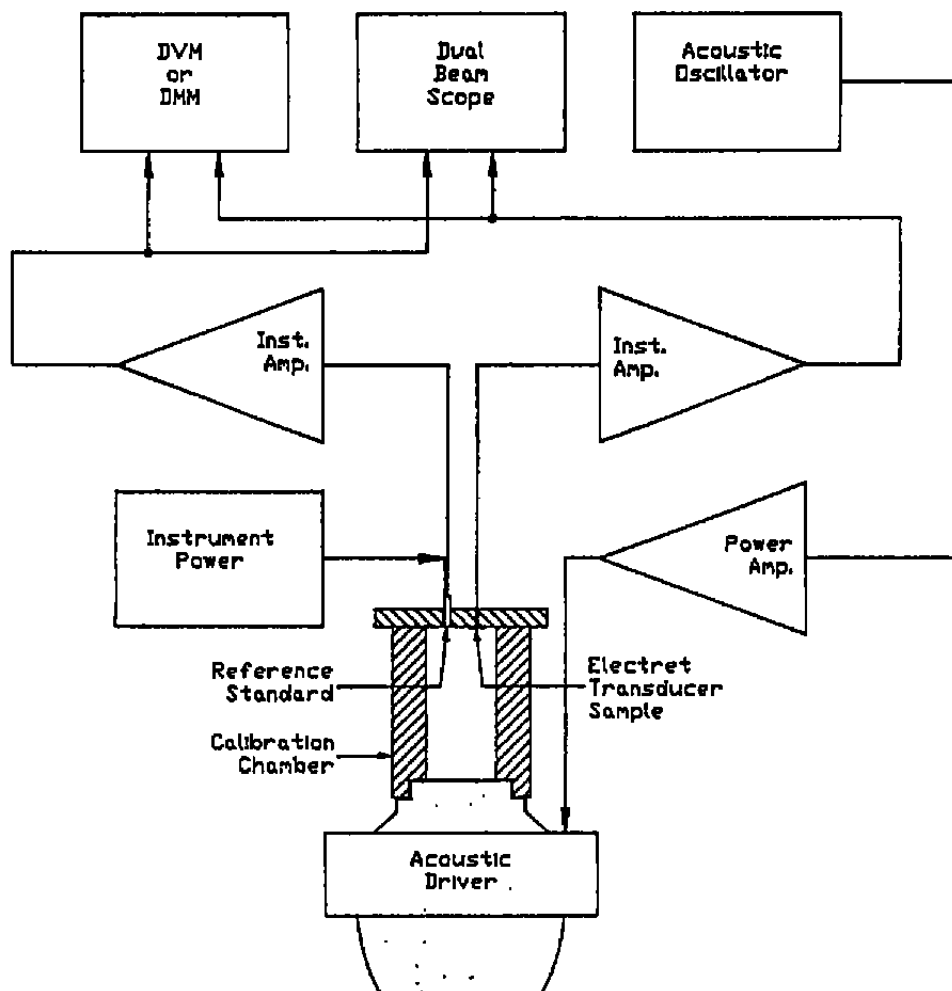
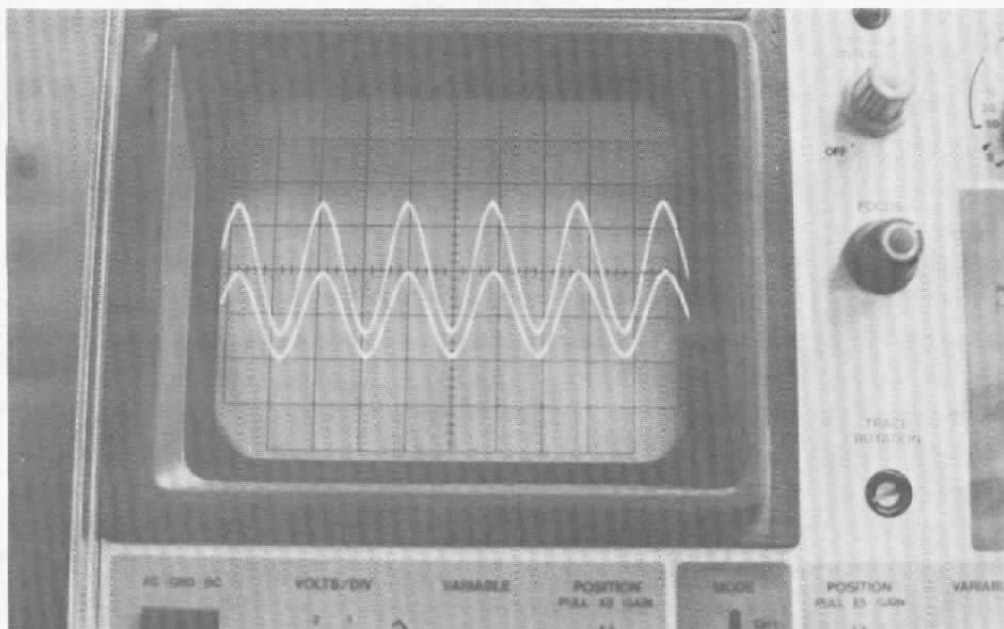Figure 18 - Transducer Element Evaluation

Figure 19 - Wave Tube Mode Monitor

mounted in a small plexiglas block and bonded to the side of
the wave tube. This microphone is connected to the inside of
the wave tube (very close to the end) by a short length of
0.062 brass tubing. The wave tube was inverted and placed
over the reference standard on the calibration plate. The
microphone monitoring the wave tube through the brass tube is
referred to as a monitor microphone. The reference standard
in the calibration plate was used to measure the true sound
pressure level at the end of the wave tube, and its
calibration transferred to the monitor microphone. Figure 21
is a photograph of the wave tube calibration transfer setup.

The wave tube was then used to calibrate the prototype
electret transition sensors. This calibration was in place;
i.e. with the prototype sensor installed on the model, and
using the actual cabling used during the wind tunnel test.
Figure 22 is a photograph of a calibration in progress. The
wave tube is placed directly over each sensor transducer
element - one at a time. The monitor microphone measures the
actual sound pressure level developed in the wave tube, and
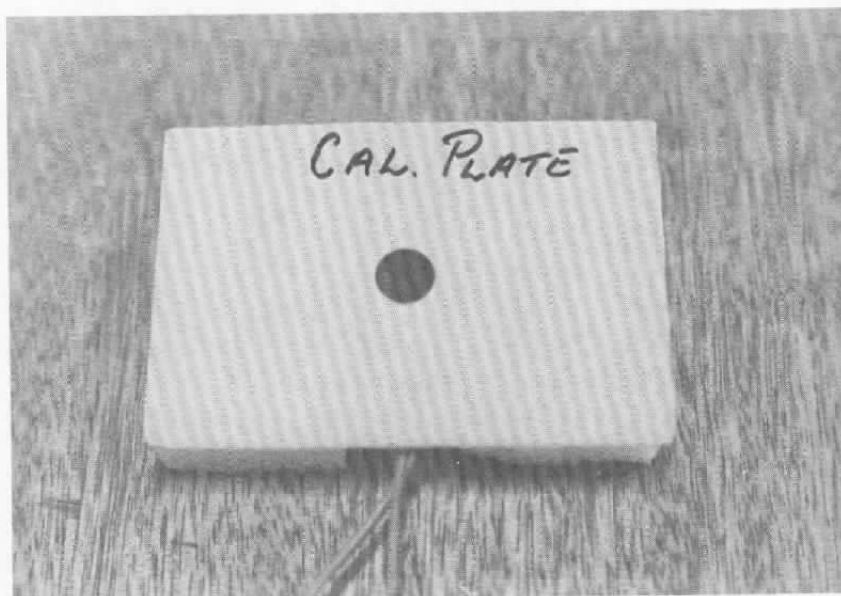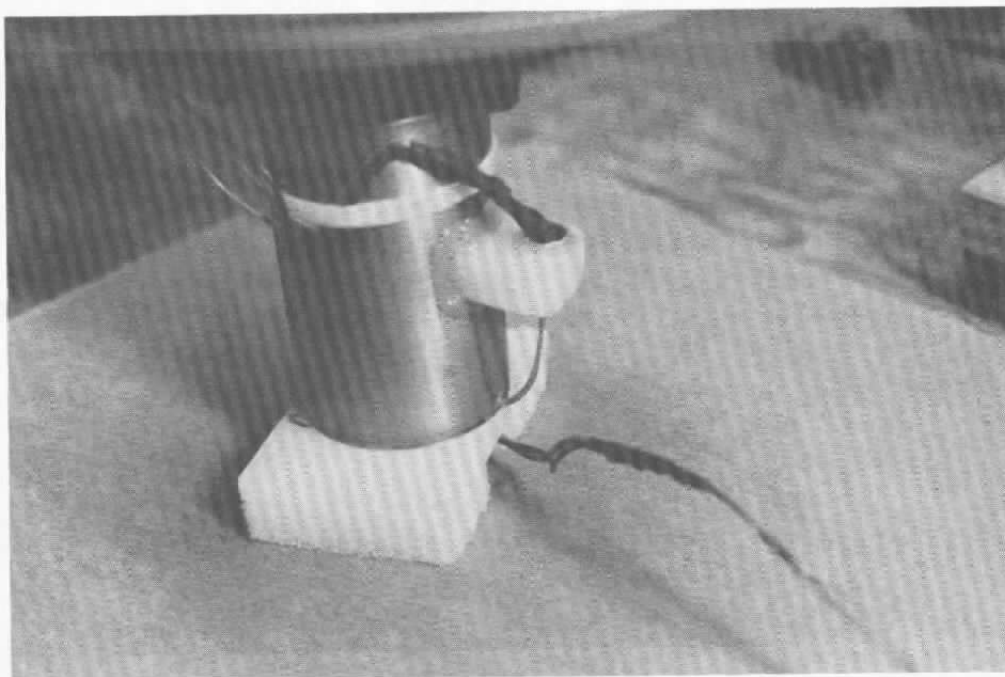provides the calibration standard.

Figure 20 - Calibration Fixture

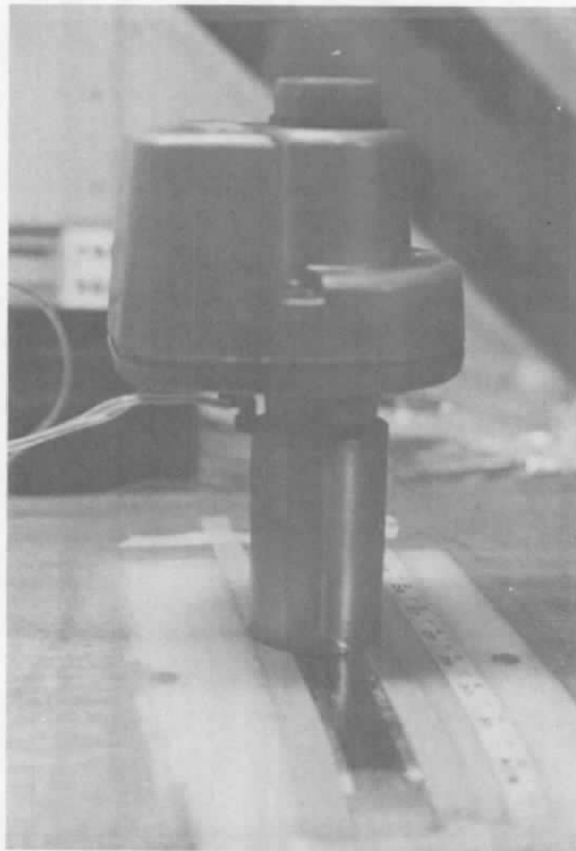Figure 21 - Transfer of Calibration @ 1 kHz

Figure 22 - Calibration of Transition Detector

The distribution of sensitivity for plate 1 is shown graphically in Figure 23. The average sensitivity is a little less than 3000 mV/psi. Note the scatter in sensitivity. Values range from a little more than 1000 mV/psi to over 8000 mV/psi. The cause of this spread in sensitivity is lack of uniformity in mask geometry and in electret tension. It was very difficult to apply the electret to the mask and maintain a uniform, wrinkle free surface. Another factor affecting the uniformity of sensitivity was the conductive adhesive used to connect the signal leads to the transducer connection pads. During thermal cycling of the adhesive appeared to swell. This was visible as tiny bumps under the film along the edges of the sensor strip. It is believed that this resulted from air trapped below the adhesive, expanding when heated. The resulting surface imperfections may have caused small variation in the mean spacing between the substrate and the electret (thereby affecting sensitivity), but it was felt that they did not jeopardize the validity of the wind tunnel test.
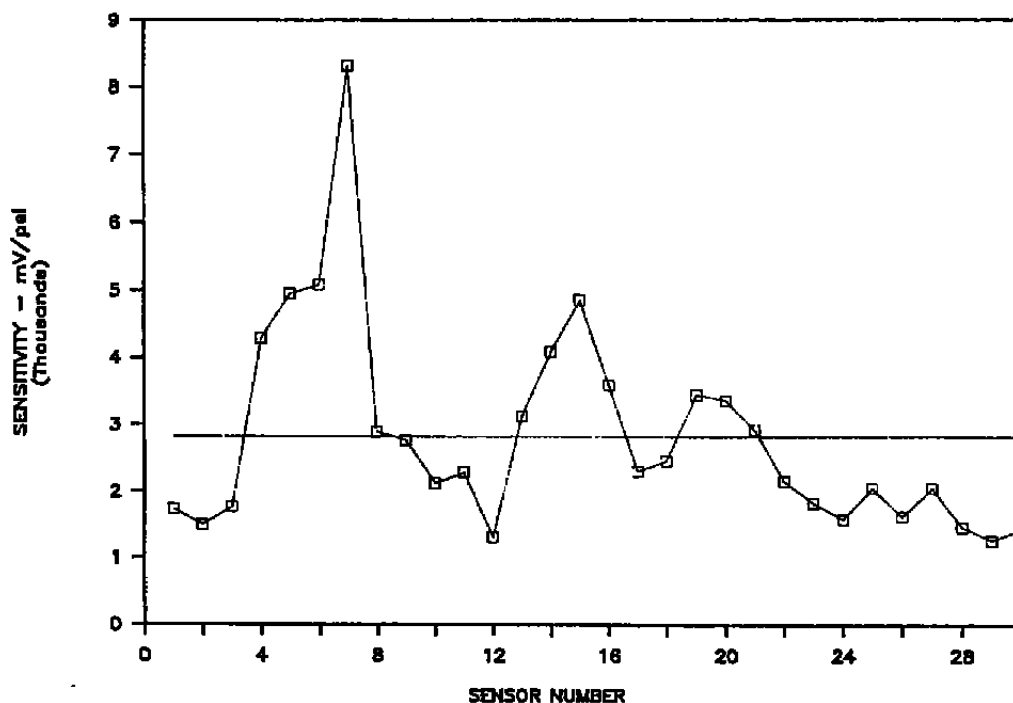
Figure 23 - Plate 1 Calibration Results

3.3 Model Design and Fabrication

The proof of concept wind tunnel test was to be conducted in the University of Missouri - Rolla 3 foot by 4 foot subsonic facility. A simple two dimensional symmetrical wing model was designed and fabricated to serve as a test bed for evaluating the electret transition sensors. The model was designed to span the tunnel from floor to ceiling. General geometry is shown in Figure 24. The leading edge is elliptical with a 2.5:1 ratio of major to minor axis.
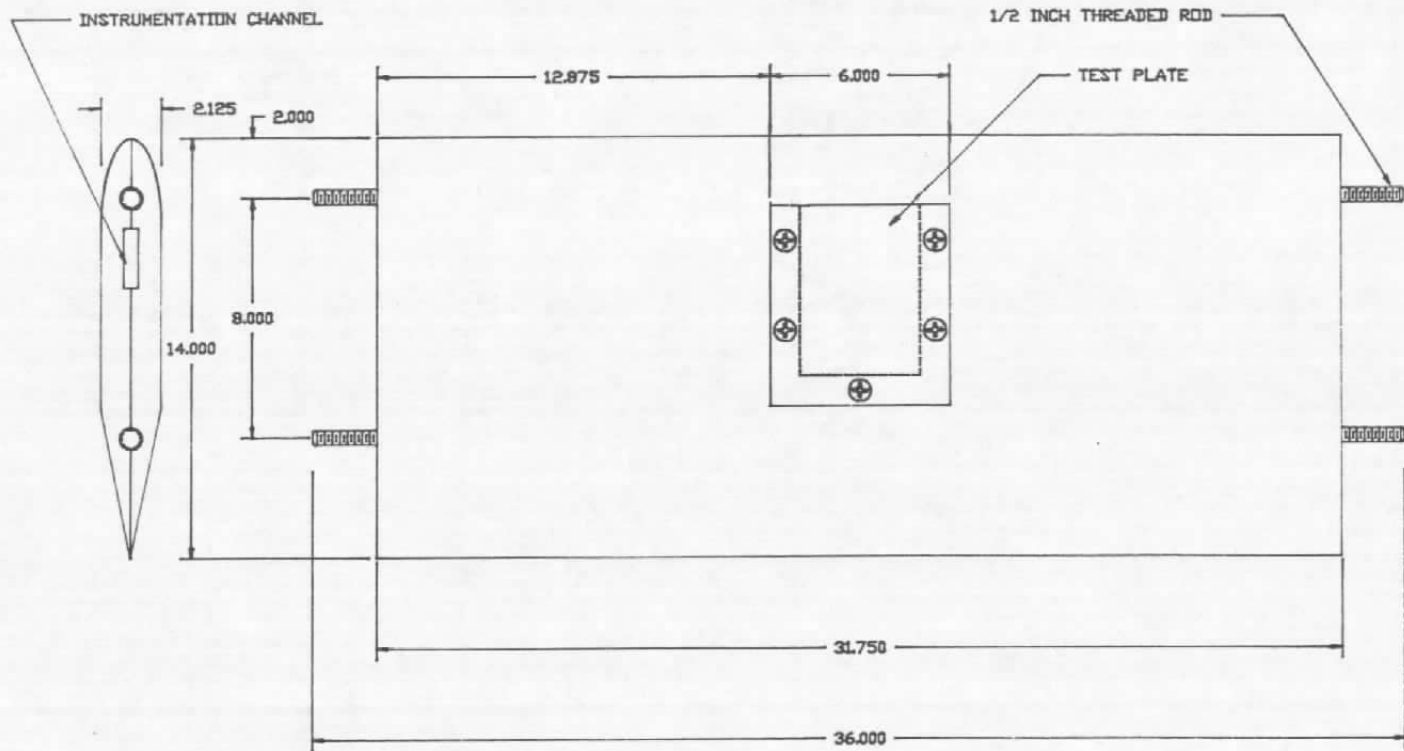
INSTRUMENTATION CHANNEL

1/2 INCH THREADED ROD

TEST PLATE

2.125

2.000

12.875

6.000

14.000

8.000

31.750

36.000

Figure 24 - General Wing Geometry

28

Model fabrication was essentially complete when review of
the basic design revealed two potential problems. The model
had a removable flat plate in the upper surface. Trial sensor
arrays were to be bonded to the plate. The plate, and sensors
could then be easily removed and/or changed without removing
the model from the tunnel. The first problem was that this
plate was tangent to the elliptical curve of the leading
edge. As a result, there was a seam between the upstream edge
of the plate and the model. If the test plate is installed
properly, and the seam waxed, no significant discontinuity
would exist. However, even small accumulations of dirt under
the plate, or a lack of repeatability in waxing could create a
lack of repeatability from one installation to the next. In
addition, this design eliminated the possibility of placing
sensors on the curved portion of the leading edge. Therefore,
it was decided to modify the test plate design.

The modified test plate wraps completely around the
leading edge of the model. The model was reworked so that the
test plate is flush with the model surface contours. This
design allows the sensors to be mounted as close to the
leading edge as desired, and eliminates the possibility of an
upstream discontinuity. The original and modified test plate
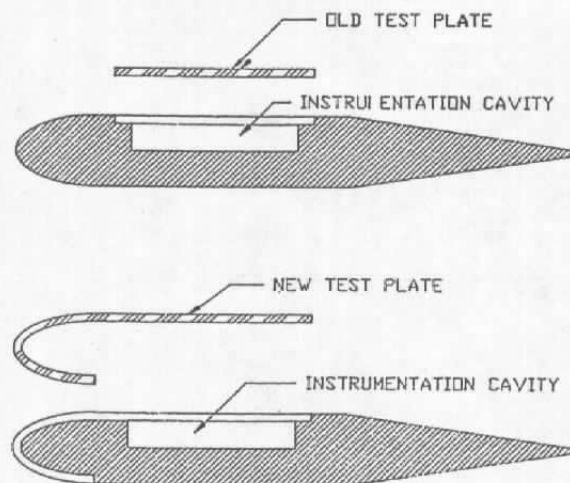installations are illustrated in Figure 25.

Figure 25 - Test Plate Modification

The second potential problem was generated by the trailing
edge of the model. The existing design called for a
relatively short trailing edge. This resulted in relatively
high expansion angles and would likely cause premature flow
separation of the aft sections of the model. The concern was
that this separation (if it occurred) may be unsteady.
Unsteady fluctuations of the separation bubble could be
communicated upstream through the boundary layer and mask the
fluctuating pressures at the sensors. This kind of masking
can be corrected if the pressure data is recorded as analog
(or rapid digital) time histories. However for the coming
feasibility test, fluctuating pressure data would be recorded
as simple time averaged RMS levels, and could not be
corrected. It was decided to lengthen the models trailing
edge. Figure 26 illustrates the original and modified
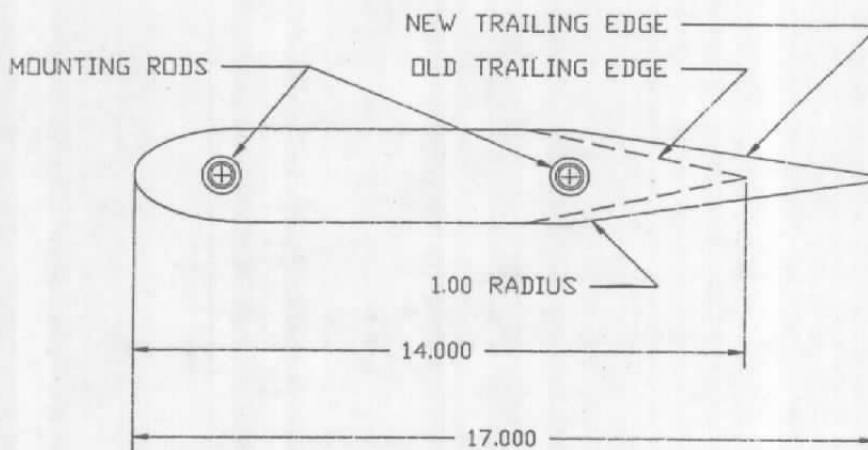designs.

Figure 26 - Trailing Edge Modification

Figure 27 is a photograph of a test plate being installed
in the model. Impedance matching electronics are located in a
cavity beneath the test plate. The signal leads from the
prototype sensor are simply plugged into a solderless
breadboard. This arrangement facilitates rapid and convenient
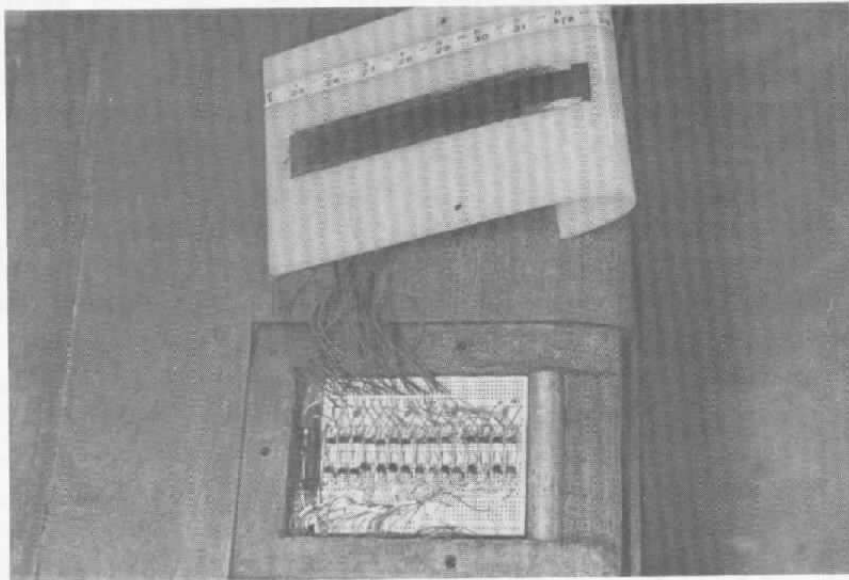sensor plate removal and replacement.

Figure 27 - Test Plate Installation

3.4 Wind Tunnel Test

The wind tunnel test was conducted in the University of
Missouri 3 foot by 4 foot subsonic facility. The test was
conducted in two distinct parts. Part 1 was concerned with
developing and verifying a conventional boundary layer probe.
The probe would be used to determine transition location in a
conventional way. For the low speeds involved in this test,
the probe interference should have minimal effect on the
transition location. The probe and electret transition
detector would be used simultaneously. Correlation of
indicated transition locations from both methods would give
conclusive evidence of the validity (or lack thereof) of the
electret transition detector concept.

Another objective of part 1 was verification of good flow quality over the model. Since only true RMS data were being recorded the effects of separation and unsteady flow phenomena (which could mask the data) could not be detected. To determine whether flow separations occurred the back side of the model was tufted. Figure 28 is a photograph of the model and tufts at q = 4 in. H2O (q = dynamic pressure). Flow was very smooth - there was no indication of flow separation at any point on the model.

A conventional boundary layer "mouse" (flattened surface total pressure probe) and a static pressure probe were attached to a remotely controlled traversing mechanism. The probes were fabricated from 0.062 brass tubing. The inlet of the mouse was flattened and ground to provide a 0.002 inch vertical capture height. The static probe was located about 0.125 inches above the model surface. The static pressure taps were aligned with the inlet of the surface mouse.

Figure 29 is a photograph of the model and boundary layer probe installation. A blank test plate was installed during part 1. No electret sensors were used. The probe (surface total and static) were traversed along the model surface while monitoring the the pressure difference. A sudden rise in pressure difference signals the onset of transition. The probe data did give a clear indication of transition. Nevertheless an attempt was made to verify the transition locations predicted from the probe data with a another conventional method - the "China Clay " method.

The China Clay method is a visual technique for finding the location of boundary layer transition. The surface of a blank test plate was painted a flat black. A lacquer was made by mixing equal parts by volume of clear lacquer, Butyl Acetate, and Butyl Alcohol. To this was added a half part of Xylene. Aluminum Silicate powder (otherwise known as Kaolin or China Clay) was then stirred in and agitated until a good sprayable consistency was obtained. This lacquer was sprayed over the flat black surface as several fine coats. Each coat was rubbed down to maintain a smooth surface. When the China Clay lacquer is dry it produces an opaque white surface. Just before starting the flow visualization run the surface was sprayed with Methyl Salicylate. The index of refraction of the Methyl Salicylate is very near that of the China Clay. As a result the China Clay lacquer becomes transparent and the black surface underneath can be seen.

The evaporation rate under a turbulent boundary layer is significantly higher than under a laminar boundary layer. Therefore the Methyl Salicylate down stream of the transition location evaporates first and the surface turns white again. The interface between the white (turbulent) and black (laminar) gives a clear visual indication of the transition location.
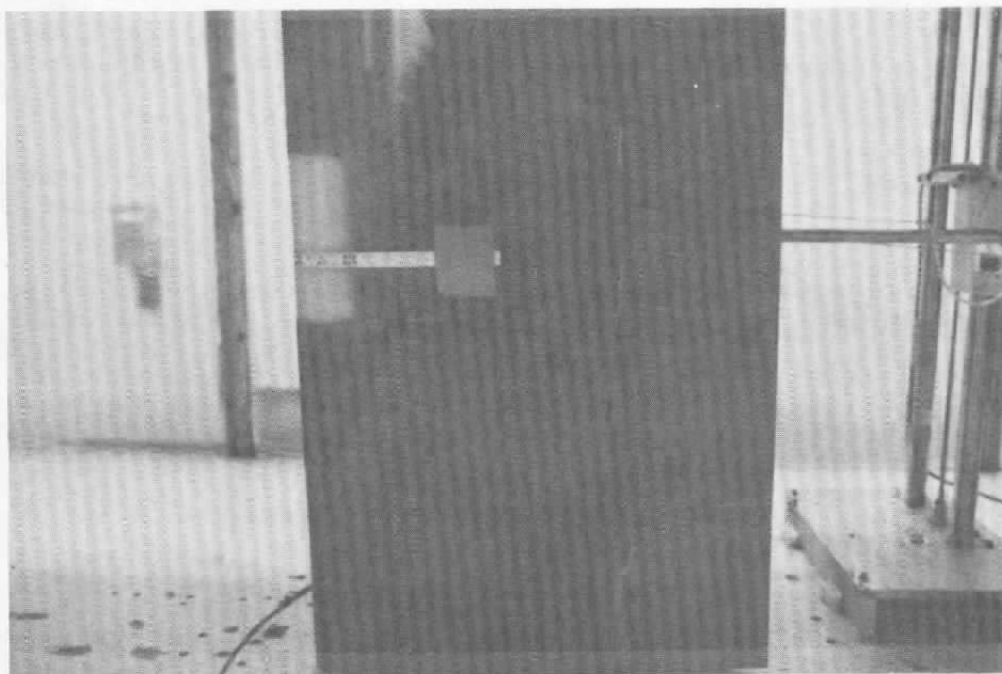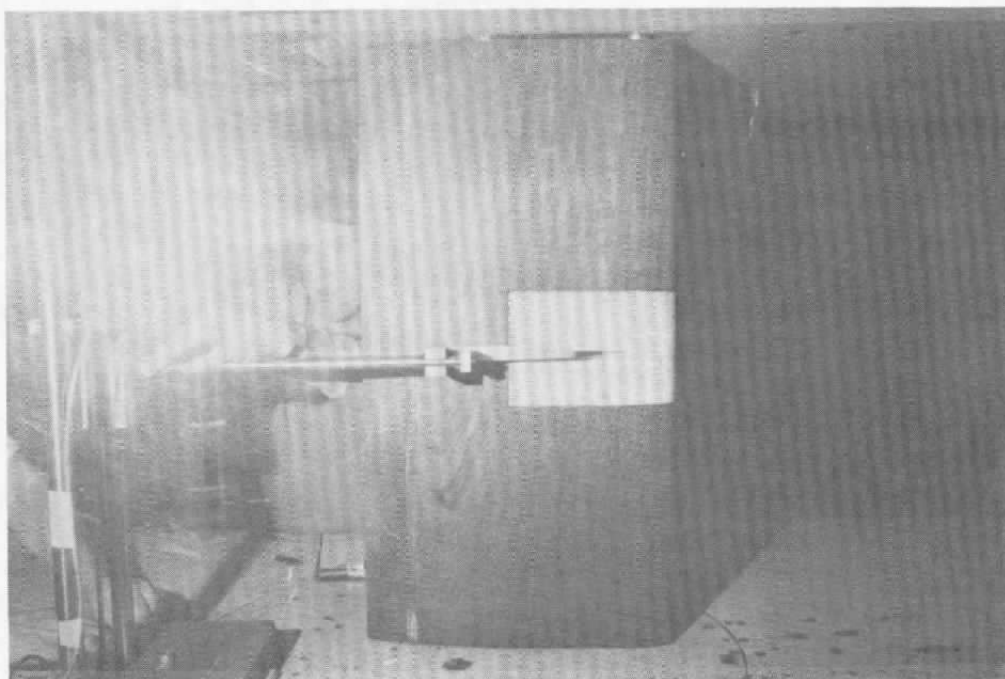
Figure 28 - Tuft Runs

Figure 29 - B.L. Probe Installation

33

After spraying with Methyl Salicylate the surface became
black - as expected. However even after 2 hours there was no
indication of the surface turning white - anywhere. The plate
was removed and set aside. Two days later the plate finally
began to slowly turn white. Time pressure precluded any
further investigation or attempt to verify the boundary layer
probe. It was necessary to proceed with part 2 - the proof of
concept testing.

All three test plates with prototype sensors as described
in the previous section were tested. Figure 30 is a
photograph showing details of the boundary layer probe and the
electret transition detector. Electret sensor data was
acquired using a computer controlled HP 3497A Data Acquisition
System and a HP 3478 digital multimeter. Boundary layer probe
pressure data was taken on a digital differential pressure
head with a resolution of 1 Pascal (about 0.00015 psi or 0.004
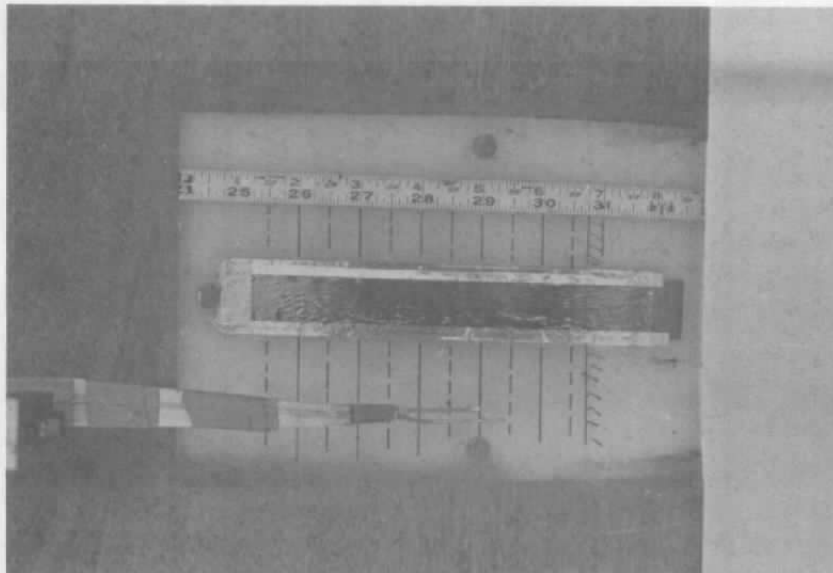inches of water).

Figure 30 - Prototype Transition Sensor & B.L. Probe

The initial series of runs consisted of three runs per
sensor configuration. Each test plate, with attached sensor,
was tested at dynamic pressures of 2, 4, and 6 inches of
water. Plate 3 (the air/elastomer matrix sensor) had
insufficient sensitivity to resolve the pressure
fluctuations. No useful data was obtained from this
prototype. This prototype might have performed well in a high
speed tunnel, where dynamic pressure is much higher and the
fluctuation intensity is correspondingly higher.

Data from plate 2 (the continuous air layer sensor) is
shown for all three runs in Figure 31. This sensor did
respond well to calibration with the standing wave tube.
However, the data obtained during the wind tunnel test does
not indicate a transition location. The sensor does respond
to the flow, but it is hard to say what exactly is being
measured. One hypothesis is that with the continuous air
layer under the electret, the electret film is simply
fluttering. What is being measured is simply an indication of
the mode shape of the surface oscillation. In any case this
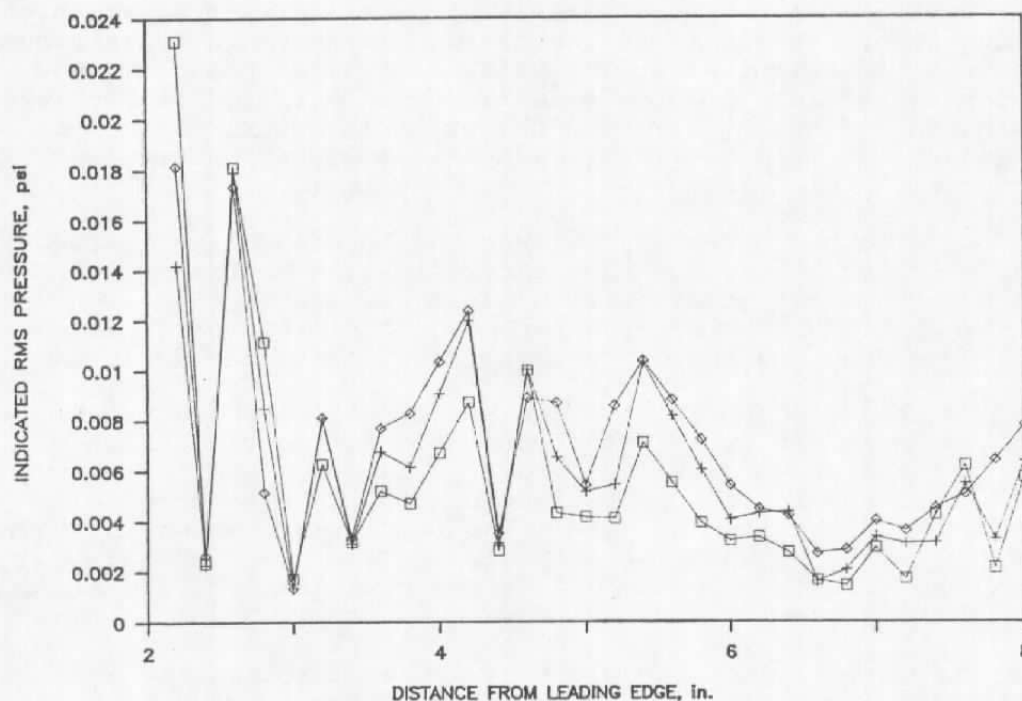prototype is not useful for determining transition location.

Figure 31 - Plate 3 @ 2", 4", and 6" H2O

Data from plate 1 (the segmented air layer sensor) did
indicate a boundary layer transition location. Data from both
the probe and the sensor were normalized and plotted
together. Figure 32 is the results of the 2 inch of water
run. The square symbols are normalized pressure difference
data from the boundary layer probe. The plus marks are
normalized fluctuating pressure data from the electret
sensor. This data is plotted as a function of distance from
the leading edge of the wing model. Following the boundary
layer probe from about 4 inches and moving aft, it can be seen

that the delta-p is initially dropping. This is believed to
be the result of recovery from the acceleration of the flow
around the leading edge. The probe data shows a minimum at
about 5.3 inches and then a rapid rise to about 6.3 inches.
This is an indication of boundary layer transition at about
the midpoint of the rise - about 5.8 inches. The electret
sensor shows an abrupt spike in measured fluctuating pressure
at that same location. A vertical line is drawn indicating
the indicated boundary layer transition location. The probe
and the electret sensor agree very well at 2 inches of water.

Figure 33 shows the same kind of data for a dynamic
pressure of 4 inches of water. Again the electret sensor and
the boundary layer probe agree as to the location of
transition. Note that as the dynamic pressure increases, both
devices indicate that the transition location moves forward.
Since increasing velocity requires a decreasing distance to
maintain a constant Reynolds number, this experimental
observation is in qualitative agreement with boundary layer
theory.

At 6 inches of water, neither the boundary layer probe nor
the electret sensor gave a clear indication of transition. It
is believed that as transition moved forward into the recovery
pressure field from the leading edge acceleration it was
pulled forward of the measurement range of either device.

To remove doubt as to the exact location of the transition
location, it was decided to induce transition at a known
station and observe the results. A boundary layer trip wire
was stretched across the surface of the plate at about 3.8
inches from the leading edge. The results are shown in Figure
34. Both the boundary layer probe and the electret sensor
indicate transition about 0.3 inches downstream of the wire.
The results seem to be conclusive.

Repeatability of the electret sensor measurements are
indicated in Figure 35. The raw (not normalized) output of
the sensor is plotted for four separate runs. The indicated
repeatability of the fluctuating pressure field is fairly
good. All four runs would indicate the same transition
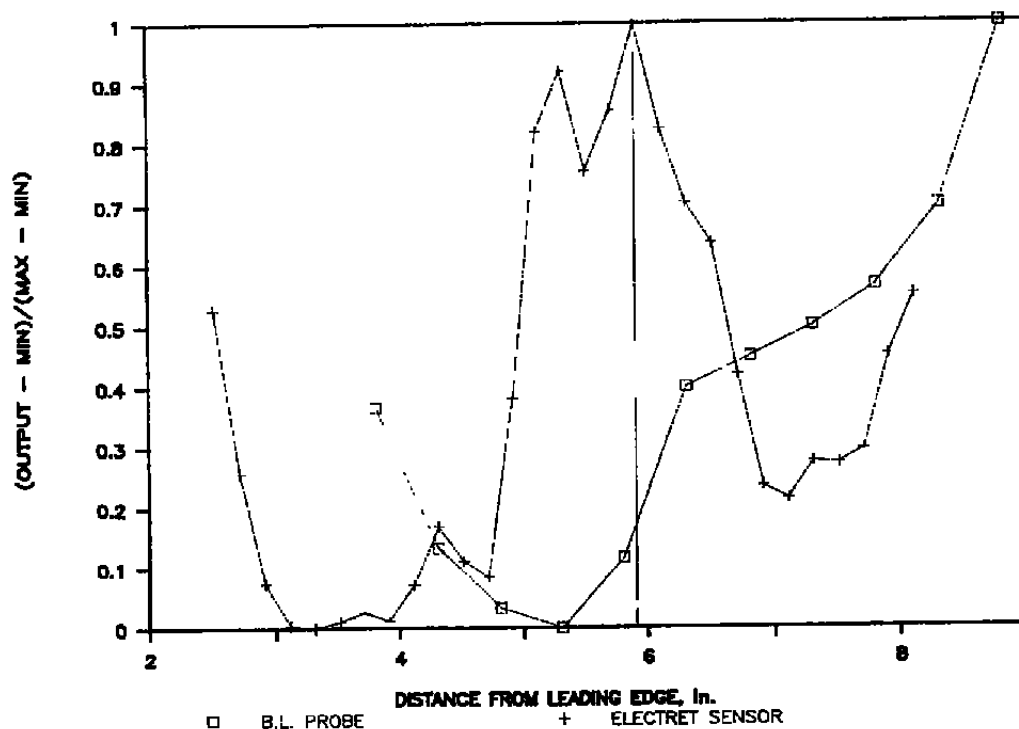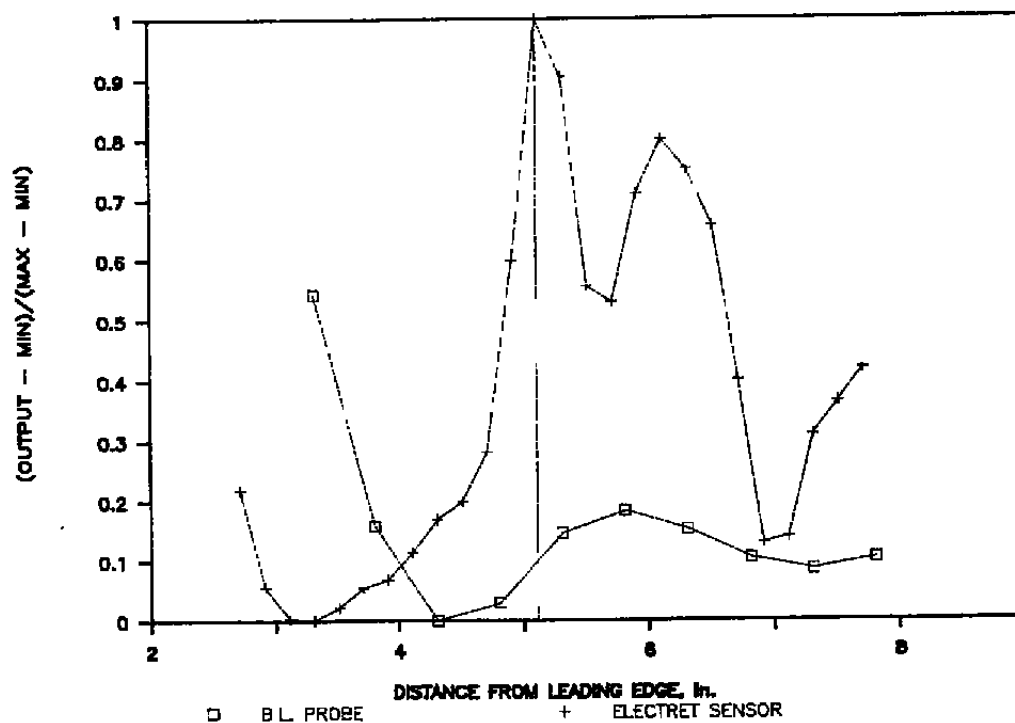location.

Figure 32 - Plate 1 @ 2" H2O

Figure 33 - Plate 1 @ 4" H2O

(PLATE 1, 4" H2O, TRIP WIRE @ 3.8")

DISTANCE FROM LEADING EDGE, in.

□ B.L. PROBE   + ELECTRET SENSOR

Figure 34 - Plate 1 With Trip Wire

(PLATE 1 — 4" H2O)

DISTANCE FROM LEADING EDGE, in.

□ RUN 7.1   + RUN 7.2   ◇ RUN 7.3   △ RUN 7.4
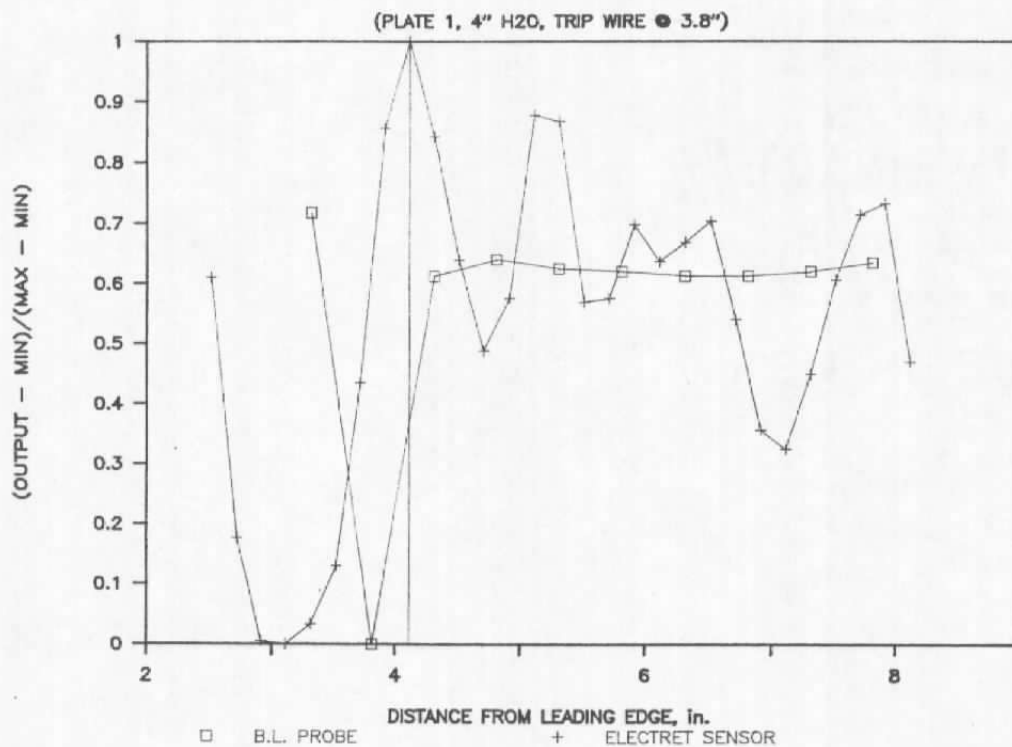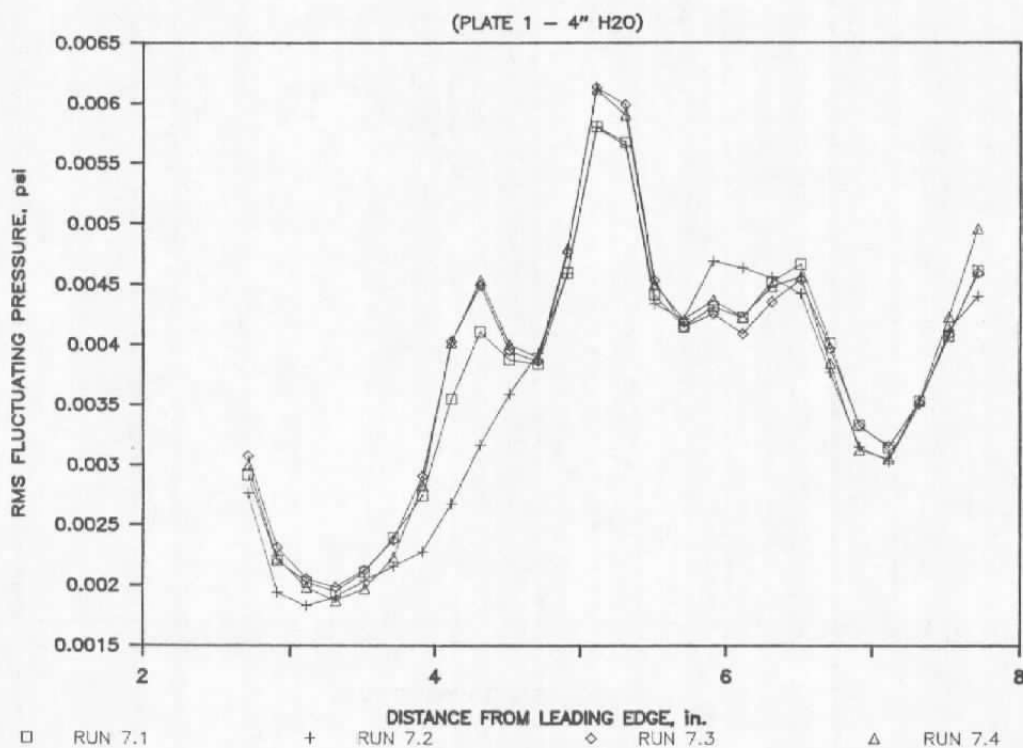
Figure 35 - Plate 1, Repeatability

4.0 CONCLUSIONS

The data seems conclusive. The feasibility of developing a thin film array of fluctuating pressure transducers for the non-intrusive location of boundary layer transition is confirmed. However, a significant amount of development remains before a production technology is achieved. The level of effort required appears to be well within the domain of an SBIR Phase II contract, and will be actively pursued.

REFERENCES

1. Morkovin, M. W., "Fluctuations and Hot-Wire Anemonetry in Compressible Flows", AGARDograph 24, Nov. 1956

2. Morkovin, M. W. and Phinney, R. E., "Extended Applications of Hot AWire Anemonetry to High-Speed Turbulent Boundary Layers", AFDSR TN-58-469, Johns Hopkins University Dept. of Aeronautics, 1958

3. Fischer, M. C., et al., "Boundary-Layer Pitot and Hot-Wire Surveys at M = 20", AIAA Journal, Vol. 9, No. 5, May 1971

4. Herzberg, G., Molecular Spectra and Molecular Structure, (D. von Nostrand Company, Inc. New York, 1950)

5. Weber, A., The Raman Effect, Vol. 2, edited by A. Anderson, (M. Dekker, Inc., New York, 1973)

6. Lapp, M., Penney, C. M., and Asher, J. A., "Application of Light Scattering Techniques for Measurements of Density, Temperature, and Velocity in Gasdynamics", Aerospace Research Laboratories Report ARL 73-0045, April 1973

7. Miles, R. B., "Resonant Laser Velocimetry", Physics of Fluids, Vol. 18, No. 6, June 1975

8. Jahoda, F. C., "Pulse Laser Holographic Interferometry", Modern Optical Methods in Gas Dynamic Research, edited by Darshan S. Dosanjh, Plenum Press, New York, 1971

9. O'Hare, J. E., "A Holographic Flow Visualization System", SPIE 14th Annual Symposium, San Francisco, California, August 1969

10. Trolinger, J. D. and O'Hare, J. E., "Aerodynamic Holography", AEDC TR-70-44, August 1970

11. Durst, F., Melling, A., and Whitelaw, J. H., Principles and Practice of Laser-Doppler Anemometry, Academic Press, London, 1976

12. Stevenson, W. H. and Thompson, H. D., The Use of the Laser Doppler Velocimeter for Flow Measurements, Proceedings, Project SQUID Workshop on Laser Doppler Velocimetry, Purdue University, West Lafayette, Indiana, March 1972

13. Thompson, H. D. and Stevenson W. H., Proceedings of the Second International Workshop on Laser Velocimetry, Purdue University, West Lafayette, Indiana, Bulletin No. 144, March 1974

14. Eckert, E. R. G., Editor, <u>Minnesota Symposium on Laser Anemometry</u>, Proceedings, University of Minnesota, Oct. 1975

15. Dougherty, Jr., N. S., "Transition Reynolds Number Compariosns in Several Major Transonic Tunnels", AIAA Paper No. 74-627, 8th Aerodynamic Testing Conference, Bethesda, Maryland, July 1974

16. Wood, G. M. et al., "Candidate Techniques for Non-Intrusive Measurement of Flight Boundary-Layer Properties", AIAA 85-0970, AIAA 20th Thermophysics Conference, Williamsburg, Virginia, June 1985

17. U.S. Patent No. 3,736,436 - "Electret Pressure Transducer", Inventor Roger C. Crites, Florissant, Mo.

18. Perlman, M. M., "Review of Phenomemological Theories of Electets", Electro Chemical Technology, Vol. 6, No. 3-4, 1968

19. Gufmann, F., "The Electret", Reviews of Modern Physics, Vol. 20, No. 3, 1948

20. Perlman, M. M. and Reedyk, C. W., "Production and Charge Decay of Film Electets", Journal of the Electro Chemical Society, Vol. 115, No. 1, 1968

21. Sessler, G. M. and West, J. E., "Foil-Electret Microphones", Journal of the Acoustical Society of America, Vol. 40, No. 6, 1966

22. Reedyk, C. WA., "An Electret Transmitter for the Telephone Set", Electro Chemical Technology, Vol. 6, No. 1-2, 1968